

**DEVELOPMENT OF SEMICONDUCTOR
NANOCRYSTALS FOR BIOTECHNOLOGICAL
APPLICATIONS**

**A Thesis Submitted to
the Graduate School of Engineering and Science of
İzmir Institute of Technology
in Partial Fulfillment of the Requirements for the Degree of**

MASTER OF SCIENCE

in Chemistry

**by
Caner ÜNLÜ**

**December 2008
İZMİR**

ACKNOWLEDGEMENTS

First of all, I want to thank my supervisor Prof. Serdar ÖZÇELİK. Without his guidance, this thesis study could not be completed. I am encouraged with his excellent supervising and endless patience during my academic program and finally able to finish this thesis. I am inspired from his knowledge and creativity in my studies and for me; he is the best example to follow as a scientist.

I would like to express my thanks to my lovely family for their motivation, continuous support and prayers. My father, Yılmaz, is the person who always supported me for my educational decisions since I was a child. My mother, Nebile, is the one who raised me with her endless love. My brother, Taner, thanks to you for being supportive and caring.

I want to thank specially to my fiancée Fatma Yelda ÖZKILINÇ. Without her love, I was not able to finish this thesis. Her endless care and her limitless support were the best motivation for me during my studies. Every time when I needed help, she was there for me to help and she gave me the best support that no one else can give. I want to thank her and her family so much for everything.

I want to thank my friends, İbrahim KARAMAN and Çağrı ÜZÜM, for their friendship in İYTE and Bilkent University, they were very helpful during my studies.

I want to thank my laboratory mates, Leyla Eral DOĞAN, Gülay DURGUN, Seda ÖZDEMİR and Burcu ALTIN for their helps, ideas and supports during my thesis study.

Assistant Prof. Mahmut KUŞ is a very special person for me. He taught me everything about synthesis and I was able to finish this study with his helps. He was very patient for me and his ideas and guidance were very important for me. I thank him so much.

I want to thank Assoc. Prof. Mustafa DEMİR, Dr. Kasım OCAKLIOĞLU, Specialist Özgür YILMAZER, Ph.D student Murat ÇOKAKLI, Ph.D student İlker ERDEM and M.Sc student Serdal OKUR for their helps during my thesis studies.

ABSTRACT

DEVELOPMENT OF SEMICONDUCTOR NANOCRYSTALS FOR BIOTECHNOLOGICAL APPLICATIONS

Semiconductor nanocrystals are very useful tools in biological applications because of their unique optical properties. In this study, synthesis and characterization of CdTe / CdS and CdSe_xS_{1-x} nanocrystals were carried out. CdSe_xS_{1-x} nanocrystals were synthesized by a modified two phase method. Highly luminescent (Quantum yield = %80) , monodisperse and face centered cubic CdSe_xS_{1-x} nanocrystals were obtained in toluene. The size of nanoparticles varies from 3.5 to 3.7 nm Ligand exchange was performed on CdSe_xS_{1-x} nanocrystals and luminescent water soluble CdSe_xS_{1-x} nanocrystals were obtained. CdTe / CdS nanocrystals were synthesized in one step and one pot by a modified method. Face centered cubic, luminescent (Quantum yield = 30%) and monodisperse CdTe / CdS nanocrystals with different sizes in a size range from 4.7 to 9.3 nm were obtained in water. Toxicity of CdTe / CdS nanocrystals was determined by MTT test. The lethal concentrations were respectively 1.0 and 15 µg/ml for PC3 and MCF7 cells. Confocal microscopy shows that the nanoparticles enter to the cytoplasm of cells.

ÖZET

YARI-İLETKEN NANOKRİSTALLERİN BİYOTEKNOLOJİK UYGULAMALAR İÇİN GELİŞTİRİLMESİ

Yarı iletken nanokristaller sahip oldukları üstün optik özellikler sayesinde biyolojik uygulamalarda kullanılmaktadır. Bu çalışmada CdTe / CdS ve CdSe_xS_{1-x} nanokristallerinin sentezi ve karakterizasyonu gerçekleştirilmiştir. CdSe_xS_{1-x} nanokristalleri değişiklik yapılmış çift fazlı sentez yöntemi ile sentezlenmiştir. Toluen içerisinde yüksek derecede ışımaya yapan (kuantum verim = %80), eşdağılımlı ve yüzey merkezli kübik yapılu CdSe_xS_{1-x} nanokristaller elde edildi. Nanoparçacıkların büyüklüğü 3.5 ile 3.7 nm arasında olacak şekilde hazırlanmıştır. CdSe_xS_{1-x} nanokristaller üzerinde ligand değişimi metodu uygulandı ve suda çözünebilen, ışımaya yapan CdSe_xS_{1-x} nanokristaller elde edildi. CdTe / CdS nanokristalleri tek basamakta su içerisinde sentezleme yöntemi ile sentezlendi. Su içerisinde ışımaya yapan (kuantum verim = %30), kübik ve eşdağılımlı, değişik büyüklüklerde (4.7 nm – 9.3 nm) CdTe / CdS nanokristaller elde edildi. CdTe / CdS nanokristallerin hücreler üzerindeki zehirlenme etkisi MTT test ile belirlendi. PC3 ve MCF 7 hücreleri için hücreler ölmeden yapılacak çalışmalarda kullanılması gereken CdTe / CdS nanoparçacık derişimleri sırasıyla 1.0 ve 15 µg/ml olarak belirlenmiştir. Konfokal mikroskopi çalışmaları ile nanoparçacıkların hücre sitoplazmasına geçtikleri belirlenmiştir.

TABLE OF CONTENTS

TABLE OF CONTENTS.....	vi
LIST OF FIGURES	viii
LIST OF TABLES.....	xii
CHAPTER 1 INTRODUCTION	1
1.1. Quantum Dots and Biotechnology.....	1
1.2. The Purpose of the study.....	3
1.3. Types of Quantum Dots	3
1.3.1. Core Type Quantum Dots including Cadmium	4
1.3.1.1. Cadmium Sulfide (CdS) Nanocrystals	4
1.3.1.2. Cadmium Selenide (CdSe) Nanocrystals	5
1.3.1.3. Cadmium Telluride (CdTe) Nanocrystals:.....	6
1.3.1.4. Cadmium Selenide Sulfide (CdSe _x S _{1-x}) Nanocrystals:	6
1.3.2. Core – Shell Type Quantum Dots including Cadmium	6
1.4. Synthesis of Quantum Dots	8
1.5. Biofunctionalization of Quantum Dots	13
1.6. Characterization of Quantum Dots	17
1.6.1. Optical Characterization.....	17
1.6.2. Structural characterization	20
1.6.3. MTT Test	23
1.6.4. Confocal Microscopy	24
1.7. Biological Applications of Quantum Dots.....	25
CHAPTER 2 DEVELOPMENT OF CdTe / CdS QUANTUM DOTS	28
2.1. Experimental	28
2.1.1. Synthesis of NaHTe as Te precursor.....	28
2.1.2. Synthesis of CdTe core nanoparticles	28

2.1.3. Synthesis of CdTe / CdS core – shell nanoparticles	29
2.2. Characterization	30
2.2.1. Optical Characterization.....	30
2.2.2. Structural Characterization:	35
2.2.3. Biological Characterization.....	38
2.2.3.1. MTT Studies	38
2.2.3.1.1. Preparation of Cell Culture.....	38
2.2.3.1.2. Treatment of Cultured Cells with Compounds and Cell Viability Assay	39
2.2.3.2. Fluorescence Confocal Microscope images.....	49
2.3. Discussion	51
2.4. Conclusion	54
CHAPTER 3 DEVELOPMENT OF CdSe _x S _{1-x} QUANTUM DOTS	56
3.1. Experimental	56
3.1.1. Synthesis of Cadmium Myristate	56
3.1.2. Synthesis of NaHSe as Se precursor	57
3.1.3. Synthesis of CdSe _x S _{1-x} nanoparticles	57
3.1.4. Ligand Exchange for CdSe _x S _{1-x} quantum dots.....	58
3.2. Characterization	58
3.2.1. Optical characterization	58
3.2.2. Structural Characterization:	65
3.3. Discussion	68
3.4. Conclusion:	70
REFERENCES	71

LIST OF FIGURES

<u>Figure</u>	<u>Page</u>
Figure 1.1. Vials of fluorescent CdSe QDs dispersed in hexane illustrate the effect of quantum confinement, in which emission wavelength depends on the size of the QD. A UV lamp serves as the excitation source. Quantum-dot sizes range from 2 nm (blue) to 8 nm (red) from left to right.....	5
Figure 1.2. Difference between emission spectra of core and core – shell structures and proposed crystal structure for CdSe / ZnS core – shell quantum dot.....	7
Figure 1.3. Structure of TOPO.....	8
Figure 1.4. Structure of Oleic Acid.....	9
Figure 1.5. Structures of 3 – Mercaptopropionic acid and Thioglycolic acid.....	10
Figure 1.6. Schematic illustration of organometallic synthesis,.....	11
Figure 1.7. A proposed mechanism for formation of CdSe in oil phase.....	12
Figure 1.8. Synthesis of CdTe nanoparticles in aqueous media.....	13
Figure 1.9. Schematic illustration of different methods for making Quantum Dots water soluble.....	14
Figure 1.10. Schematic illustration of ligand exchange.....	15
Figure 1.11. Schematic illustration of silica encapsulating.....	16
Figure 1.12. Change in fluorescence and UV – Vis Spectra due to CdS quantum dot growth.....	18
Figure 1.13. Detection of Stokes shift.....	19
Figure 1.14. XRD patterns of the “nano-onions” with CdS cores capped alternately by CdSe and CdS shells. Vertical lines indicate pure CdSe and CdS reflections (top: zinc blend, CdSe; bottom: zinc blend, CdS).....	21
Figure 1.15. TEM image of different sized quantum dots.....	22
Figure 1.16. AFM image of PbTe quantum dots.....	23
Figure 1.17. MTT reduction scheme.....	24
Figure 1.18. Confocal micrograph of peritoneal macrophage from mouse incubated with CdTe QDs-labeled anti-MHC-II.....	25
Figure 2.1. Schematic Illustration of Synthesis of CdTe.....	29
Figure 2.2. Structure of Thiourea.....	29

Figure 2.3.Schematic illustration of Synthesis of CdTe / CdS core – shell quantum dots (QD).....	30
Figure 2.4.Normalized fluorescence spectrum of CdTe / CdS nanoparticles synthesized at different time intervals.....	31
Figure 2.5.Luminescence image of CdTe / CdS nanoparticles under UV lamp.....	32
Figure 2.6.Temporal evolution of fluorescence peaks of CdTe / CdS nanoparticles	32
Figure 2.7.UV – Vis spectra of green, yellow and red emitting CdTe / CdS nanoparticles.....	33
Figure 2.8.Fluorescence spectra of green, yellow and red emitting CdTe / CdS nanoparticles.....	33
Figure 2.9.XRD spectra of yellow and red emitting CdTe / CdS nanoparticles, red dots hkl indices of cubic bulk CdTe (bottom), black dots hkl indices of cubic bulk CdS (top)	35
Figure 2.10.DLS analysis of yellow CdTe / CdS nanocrystals	36
Figure 2.11.DLS analysis of yellow CdTe / CdS nanocrystals	37
Figure 2.12.MTT results for green CdTe / CdS quantum dots in MCF7 cells for 1 day.....	40
Figure 2.13.MTT results for green CdTe / CdS quantum dots in MCF7 cells for 2 days	40
Figure 2.14.MTT results for green CdTe / CdS quantum dots in PC3 cells for 1 day.....	41
Figure 2.15.MTT results for green CdTe / CdS quantum dots in PC3 cells for 2 days	41
Figure 2.16.MTT results for yellow CdTe / CdS quantum dots in MCF7 cells for 1 day.....	42
Figure 2.17.MTT results for yellow CdTe / CdS quantum dots in MCF7 cells for 2 days	42
Figure 2.18.MTT results for yellow CdTe / CdS quantum dots in PC3 cells for 1 day.....	43
Figure 2.19.MTT results for yellow CdTe / CdS quantum dots in PC3 cells for 2 days	43
Figure 2.20.MTT results for red CdTe / CdS quantum dots in MCF7 cells for 1 day.....	44

Figure 2.21.MTT results for red CdTe / CdS quantum dots in MCF7 cells for 2 days	44
Figure 2.22.MTT results for red CdTe / CdS quantum dots in PC3 cells for 1 day	45
Figure 2.23.MTT results for red CdTe / CdS quantum dots in PC3 cells for 2 days	45
Figure 2.24. MTT results for CdCl ₂ in MCF7 cells for 1 day	46
Figure 2.25. MTT results for thiourea in MCF7 cells for 1 day	46
Figure 2.26. MTT results for CdCl ₂ in PC3 cells for 1 day	47
Figure 2.27.MTT results for Thiourea in PC3 cells for 1 day	47
Figure 2.28.Colored Fluorescence confocal microscope image of green light emitting CdTe / CdS in liver cancer cells	49
Figure 2.29.Colored Fluorescence confocal microscope image of yellow light emitting CdTe / CdS in liver cancer cells	50
Figure 2.30.Colored Fluorescence confocal microscope image of red light emitting CdTe / CdS in liver cancer cells	50
Figure 3.1.Structure of myristic acid	56
Figure 3.2.Structure of Cadmium Myristate	56
Figure 3.3.Schematic Illustration of Synthesis of CdSe _x S _{1-x}	58
Figure 3.4.Fluorescence spectrum of CdSe _x S _{1-x} nanoparticles synthesized at different time intervals (from 0.5 hour to 13 hours)	59
Figure 3.5.Temporal evolution of fluorescence peaks of CdSe _x S _{1-x} nanoparticles	59
Figure 3.6.Fluorescence spectrum of CdSe _x S _{1-x} nanoparticles synthesized at different time intervals (from 0.5 hour to 15 hours)	60
Figure 3.7.Temporal evolution of fluorescence peaks of CdSe _x S _{1-x} nanoparticles	60
Figure 3.8.UV – vis spectra of CdSe _x S _{1-x} quantum dots	61
Figure 3.9. Fluorescence spectra of CdSe _x S _{1-x} quantum dots	61
Figure 3.10.Luminescence image of CdSe _x S _{1-x} nanoparticles under UV lamp	62
Figure 3.11.Fluorescence and UV – Vis spectra of CdSe _x S _{1-x} nanoparticles (Emission 525 nm)	62
Figure 3.12.Fluorescence wavelength change after ligand exchange	64
Figure 3.13.Fluorescence intensity change after ligand exchange	64
Figure 3.14.TEM images of CdSe _x S _{1-x} nanoparticles (20 nm scale)	65
Figure 3.15.TEM images of CdSe _x S _{1-x} nanoparticles (5 nm scale)	66

Figure 3.16. XRD spectra of purple, blue and green emitting $\text{CdSe}_x\text{S}_{1-x}$ nanoparticles, red dots hkl indices of cubic bulk CdSe (bottom), black dots hkl indices of cubic bulk CdS (top)..... 66

LIST OF TABLES

<u>Table</u>	<u>Page</u>
Table 2.1. Photophysical Properties of CdTe / CdS nanoparticles.....	34
Table 2.2. Size Analysis of CdTe / CdS Nanoparticles with XRD	36
Table 2.3. Size determination of CdTe / CdS nanoparticles from XRD, UV – vis spectroscopy and DLS.....	38
Table 2.4. ICP – MS analysis of CdTe / CdS nanoparticles.....	38
Table 2.5. MTT Test results for CdTe / CdS nanoparticles, CdCl ₂ and Thiourea in MCF7 and PC3 Cells.....	48
Table 3.1. Photophysical properties of CdSe _x S _{1-x} nanocrystals.....	63
Table 3.2. Optical Changes after ligand exchange	64
Table 3.3. Size determination of CdSe _x S _{1-x} nanoparticles from TEM, XRD and UV – vis Spectroscopy.....	67

CHAPTER 1

INTRODUCTION

1.1. Quantum Dots and Biotechnology

Swift developments in nanoscience have allowed scientists to develop nanomaterials that have highly controlled and unique optical properties. Lately, biologists have started to use these nanomaterials in different applications such as diagnosis of diseases, gene therapies, etc... Joining of biomaterials with semiconductor quantum dots or metal nanocrystals improves the impact of biophotonics and bioimaging in biological and medical sciences. (Wang, et al. 2005)

Quantum dots are defined as nanometer-scale semiconductor crystals comprised of groups II–VI or III–V elements, and are described as particles with physical dimensions smaller than the exciton Bohr radius. (Jamieson, et al. 2007) Nanomaterials' properties can be tuned by controlling their physical size. In the nanometer size regime, new mesoscopic phenomena characteristic of this intermediate state of matter, found in neither bulk nor molecular systems, comes out. Quantum dot's physical properties strongly depend on crystal size, due to quantum confinement effect. (Bawendi, et al. 2000)

The spatial confinement of excitations, electronic and vibrational, dominate the physical properties of semiconductor nanocrystals.(Bawendi, et al. 1994) The most striking property of semiconductor quantum dots is their ability to change optical properties by controlling their size. When a bulk semiconductor crystals' size is reduced, the surface area / volume ratio increases and surface structure affects optical and electronic properties strongly. Furthermore, the crystal's electronic properties stop behaving as bulk structure. This behaviour is a result of quantum confinement effects, the behaviour of electrons in a particle due to spatial restrictions.

In a semiconductor, electron moves from valence band to conduction band due to light absorption. The energy required for excitation of electron is indicated by the energy band gap. The moving electron's motion is accepted as moving through a

“hole”, and this electron – hole pair becomes electrostatically bound, creates an exciton, which is defined by a distance known as the Bohr Radius. When the excited electron loses its excess energy in the conduction band, it returns to valance band and remerges with the hole. Light forms due to combination of electron and hole pair.

As an exciton forms in a spatially confined in a region smaller than the bohr radius, the quantum dot’s band gap increases since much more energy is needed to confine the exciton. So, blue shift occurs in light that occurred due to energy loss of electron – hole pair, which means light occurs in a shorter wavelength (higher energy). That means, as quantum dot’s size decreases, the absorption and emission wavelengths shifts to blue, lower wavelength.

The minimum energy required to form an exciton can be ascribed to the bulk band gap energy and the confinement energy for the electron carriers in a potential well. The whole confinement energy for the exciton can be described by “particle in a box” system:

$$E_{well} = \frac{h^2}{2md^2} \quad (1.1)$$

where h is planck’s constant, d is diameter, m is reduced mass of exciton.

However, coulombic interactions also affect exciton energy, which is described as:

$$E_{coul} = \frac{-1.8e^2}{2p\epsilon\epsilon_0d} \quad (1.2)$$

where e = electron’s charge (C), ϵ_0 = dielectric constant and ϵ = permittivity constant. Combining these equations may give an idea to calculate the energy band gap of a quantum dot.

$$E(\text{dot}) = E_g (\text{bulk}) + E_{well} + E_{Coul} \quad (1.3)$$

$$E = E_g + \frac{h^2}{2md^2} - \frac{1.8e^2}{4p\epsilon\epsilon_0d} \quad (1.4)$$

This is known as effective mass approximation. Both coulombic and confinement terms depend on size, and when the quantum dot's size is very small, confinement term becomes the dominant term. (Juandria V. Williams 2008)

Recently, quantum dots have been used in biotechnology efficiently. After Alivisatos et al. (1998) and Nie et al. (1998) showed that quantum dots can be used in biotechnology. Generally, quantum dots are synthesized in apolar solvents such as toluene, heptanes, etc.... However, quantum dots must be water soluble to be used in bioimaging. For that reason, researchers try to make water soluble quantum dots with different methods, such as ligand exchange and one – pot synthesis (Sharma, et.al 1998) With their excellent optical properties, quantum dots are used as labeling agents in bioimaging.

Different from quantum dots, also organic dyes can be used as fluorophores in biological applications. However, in bioimaging, quantum dots have overcome many of restrictions of organic dyes, such as poor photostability, low quantum yield, insufficient in vitro and in vivo stability, etc... By help of unique optical properties of quantum dots, they can be developed for real time and deep tissue imaging via optical routes. (Sharma, et.al 1998)

1.2. The Purpose of the Study

The purpose of the study is to develop a method to synthesize and characterize water soluble quantum dots for biotechnological applications. These applications may be bioimaging in cells by using unique optical properties of quantum dots.

1.3. Types of Quantum Dots

Quantum dots differ in many ways. To classify them according to one condition is not a logical way; however there are some distinct terms that quantum dots are grouped in. Quantum dots can be classified in two groups according to their atomic arrangement in crystal structure such as core types and core – shell types. A core type quantum dot consists of two or three atoms. However, coating the core of quantum dot, which means surrounding core with a shell consisting of different kind of atoms, causes a great enhancement in optical properties, such as quantum yield and photostability, and

notable improvements on biological properties, such as toxicity. This type of quantum dots is called core – shell type quantum dots. There are different kinds of core and core – shell type quantum dots depending on atom type; CdS, CdSe, CdTe, ZnS, PbS, GaInP₂, CdHgTe, CdSexS_{1-x}, CdSe / ZnS, CdSe / CdS, CdTe / CdS ... Between these quantum dots, quantum dots including cadmium have very unique and tunable optical properties. Because of these properties, researchers show great interest in these types of quantum dots.

1.3.1. Core Type Quantum Dots including Cadmium

In early studies, Bawendi et.al synthesized monodisperse CdS, CdTe and CdSe nanocrystals successfully (Bawendi, et al. 1994). Also, recently CdSe_xS_{1-x} and CdHgTe alloyed monodisperse nanocrystals are synthesized (Qian, et.al 2007, Jang, et.al 2003). Each of these nanocrystals has different and unique properties and is used in many research areas such as LEDs, solar cells, biological markers (Alivisatos, et al. 1994, Alivisatos, et al. 1997, Alivisatos, et al. 1998, Alivisatos, et al. 2002, Alivisatos, et al. 1999, Bawendi, et al. 2000, Bawendi et al. 2002, Nie et al. 1998).

1.3.1.1. Cadmium Sulfide (CdS) Nanocrystals

Amongst quantum dots including cadmium, CdS is the easiest one to be synthesized. High temperatures and high pressures are not required for the synthesis CdS . There are several types of methods to synthesize CdS; organometallic route, two phase method, solvothermal method, etc... Emission spectrum of CdS nanoparticles may vary between 350 nm and 500 nm, which means CdS can emit colors between violet and green. CdS nanoparticles are used in many research areas including light emitting diodes, solar cells, lasers and biological markers. (Alivisatos, et al. 1994, Alivisatos, et al. 1997, Alivisatos, et al. 1998, Alivisatos, et al. 2002, Alivisatos, et al. 1999, Bawendi, et al. 2000, Bawendi et al. 2002, Nie et al. 1998).

1.3.1.2. Cadmium Selenide (CdSe) Nanocrystals

CdSe quantum dots are the most commonly used and investigated quantum dots. However, to synthesize CdSe quantum dots is somewhat complicated when it is compared to synthesize of CdS quantum dots, usually higher temperature and higher pressure is needed to synthesize. It is impossible to synthesize CdSe nanocrystals in the presence of O₂ since Se precursors are easily oxidized by air. In early studies, Alivisatos produced CdSe by organometallic synthesis method (Alivisatos, et al. 1992). Bawendi et. al. synthesized CdSe with a different kind of organometallic synthesis route (Bawendi, et al. 1994). Lately, Pan et.al. synthesized CdSe quantum dots with two – phase method. (Pan, et al. 2005) Cadmium selenide is interesting because it has unique optical properties in the visible spectrum. Through strict dimensional control, QDs can be produced to emit narrow color spectra that can be clearly distinct from one another at the full-width half maximum of the peak emission and have typical full-width half-maxima of only 25nm to 30nm. Because the color spectra do not overlap, one can increase the number of distinct colors, as compared to organic dyes, that are being detected simultaneously.(Figure 1.1)



Figure 1.1. Vials of fluorescent CdSe QDs dispersed in hexane illustrate the effect of quantum confinement, in which emission wavelength depends on the size of the QD. A UV lamp serves as the excitation source. Quantum-dot sizes range from 2 nm (blue) to 8 nm (red) from left to right. (Source: Dabbousi, et al. 1997)

CdSe nanoparticles are used in many research areas such as biomedical imaging applications, laser diodes, etc... (Alivisatos, et al. 1994, Alivisatos, et al. 1998)

1.3.1.3. Cadmium Telluride (CdTe) Nanocrystals:

In early studies, synthesis of CdTe was subset of synthesis of CdSe and a little information was gathered about CdTe nanoparticles. Bawendi et.al. and Talapin et.al made early studies about CdTe quantum dots (Bawendi, et al. 1994&Talapin, et al. 2002). However, easy synthesis of CdTe in aqueous solutions has been called attention by researchers and several important studies have been performed on CdTe nanocrystals (Gaponik, et al. 2002, Qian, et al. 2007, Cho, et al. 2007, Zhong, et al. 2008). Gaponik et.al. synthesized CdTe nanocrystals in aqueous media in one step, with non – expensive materials such as Al_2Te_3 , (Gaponik, et al. 2002). Ren et.al. synthesized CdTe nanocrystals in aqueous media in one step and deposited it with Hg to obtain near infra – red color (Qian, et.al 2007). Lately, CdTe quantum dots have been used for biological applications. However, high toxic effects of both cadmium and tellurium limit the utilization of CdTe quantum dots in biological applications. (Cho, et al. 2007)

1.3.1.4. Cadmium Selenide Sulfide ($CdSe_xS_{1-x}$) Nanocrystals:

$CdSe_xS_{1-x}$ is an alloyed type core nanocrystal, which is not studied widely and still has terms to be developed. It is not called a core – shell type quantum dot because both S and Se precursors are added together at the same time during synthesis, however because of the difference in reaction rates of S and Se, inner side of crystal structure is assumed to be S or Se rich depending on their reaction rate. This alloyed type quantum dots differ from other core type quantum dots in some ways. Its optical properties depend on the ratio of S to Se in crystal structure (Jang, et.al 2003). Also, Jang et.al synthesized and observed electroluminescence of $CdSe_xS_{1-x}$ quantum dots, and showed that this quantum dot can be used in preparation of light emitting devices (Jang, et.al 2003).

1.3.2. Core – Shell Type Quantum Dots including Cadmium

After synthesizing core quantum dots, scientists paid attention to develop their physical and biological properties. Since atoms on large surface area could not be fully

coordinated, dangling bonds of nanocrystal surface generated non-radiative decay energy levels to reduce quantum yield. However, growing a thin inorganic shell epitaxially on the surface of the core causes surface passivation and makes crystal structure less defective. The basic logic in core – shell synthesis is, first to grow a kind of core nanocrystal, then to grow a different kind of inorganic layer around core which has close crystal structure of core material. This thin shell around core, improves optical properties of core structure dramatically. (Figure 1.2)

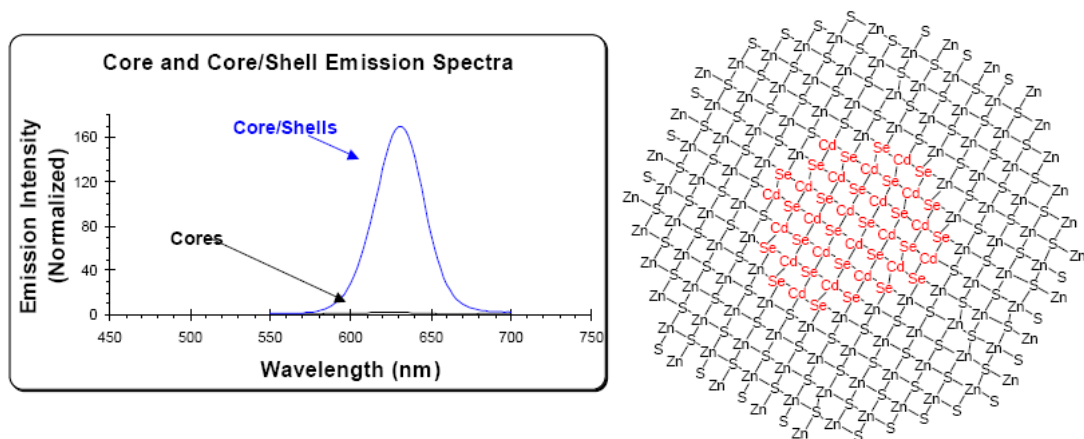


Figure 1.2. Difference between emission spectra of core and core – shell structures and proposed crystal structure for CdSe / ZnS core – shell quantum dot.(Source: Nanobiotechnology Forum – 2003, Quantum Dot Corporation.)

For CdSe/CdS and CdSe/ZnSe core-shells, the lattice structures of core and shell are compatible with each other. For CdSe/CdS nanocrystals, CdS grows epitaxially and coherently around CdSe, as a result of the low concentration of defects in the shell, CdSe/ CdS and CdSe/ZnSe nanocrystals exhibit very high fluorescence quantum efficiencies, up to 80-90% (Talapin, et al. 2004).

Ren et.al. synthesized CdHgTe alloyed quantum dots and obtained nanocrystals that have emission spectra close to infrared. By coating this CdHgTe alloyed quantum dots with a CdS shell, they also improved photostability of CdHgTe alloyed quantum dots and developed an alternative near – infrared emitting labeling source for biolabeling applications (Qian, et.al 2007).

There are studies on core – shell – shell and core – shell – shell – ... – shell quantum dots (Talapin, et al. 2004 & Pan, et al. 2006). The main reason for coating

surface with more shell structures is basically to get more advanced quantum dots. By covering core – shell structure with another shell, improving quantum yield, stability and robustness of luminescent nanocrystals were aimed. However, it is not easy to control the shell thickness of middle and outer shell, so studies cannot be interpreted easily (Talapin, et al. 2004). Also, adding more shell does not always improve core structure's photophysical properties (Pan, et al. 2006).

1.4. Synthesis of Quantum Dots

Researchers tried many different ways to synthesize quantum dots in the past years. Naturally, many different synthesis types are developed for synthesizing these materials. Since this synthesis can be considered as growth of a crystal structure, it is very important to control temperature during synthesis. However, it is also very important to grow monodisperse nanocrystals, otherwise optical properties of these nanocrystals drops dramatically. By controlling only temperature and pressure, to synthesize monodisperse quantum dots is extremely difficult, because quantum dots can accumulate in an instant, bulk crystal structures occur. However, by using organic surfactants, monodisperse quantum dots can be readily synthesized.

The surfactants are tailored to meet specific parameters such as water-solubility, chemical reactivity, or to keep particles from agglomerating. The most common capping structures to use are those that also act as the solvent in which the organo-metallic reaction occurs. Organometallic synthesis method requires high temperature (300 °C). There are many organic solvents with high boiling point; however, only a few have been tested. Of these, trioctylphosphine oxide, TOPO, (Figure 1.3) has been thoroughly used over a wide range of production and subsequent environmental applications.

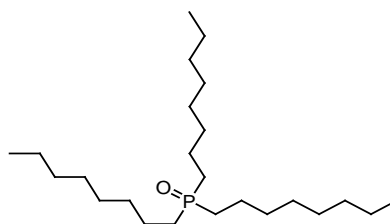


Figure 1.3. Structure of TOPO

TOPO is widely used in quantum dot synthesis, most of semiconductor precursors dissolve in TOPO and TOPO also acts as a medium for the reaction. However, Pan et.al indicated that TOPO may cause trap states on the surface, so that emission spectrum of quantum dot may have a broad shoulder, resulting from lower capping densities (Pan, et al. 2004). Instead of TOPO, also oleic acid may be used as surfactant.

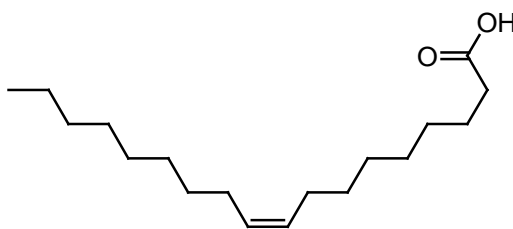


Figure 1.4. Structure of Oleic Acid

Oleic acid is mono unsaturated omega – 9 fatty acid found in various animal and vegetable sources. (Figure 1.4) This long carbon chained fatty acid is widely used as capping agent in quantum dot synthesis. Oleic acid easily dissolves in apolar solvents such as toluene and heptane, that property make oleic acid very useful in quantum dot synthesis. Oleic acid surrounds quantum dots better and yields to narrower photoluminescence peaks, which mean greater monodispersity, and trap states decreases with oleic acid when it is compared to TOPO. Oleic acid is a cheap organic matter that can be achieved easily. However, excess oleic acid makes difficult ligand exchange.

However, the capping agents that mentioned above cannot be dissolved in water. For biological applications, quantum dots must be dissolved in water. Generally, 3 – Mercaptopropionic acid and Thioglycolic acid are used for this purpose (Figure 1.5). These capping agents bind quantum dots from thiol group (- SH) and free carboxylic groups allow 3 – MPA or TGA capped quantum dots to be able to dissolve in aqueous media.



Figure 1.5. Structures of 3 – Mercaptopropionic acid and Thioglycolic acid

In early studies, Bawendi et.al synthesized monodisperse quantum dots by organometallic hot schlenk method (Bawendi, et al. 1994). In this method, airless media and very high temperature are the most important conditions in synthesis. Cadmium precursor and selenium, tellurium or sulfur precursors are dissolved in surfactant (TOPO or TOP generally) under nitrogen or argon atmosphere, at very high temperature (around 300 °C). At high temperature, nucleation occurs and lowering temperature a little (around 280 °C), growth starts and monodisperse quantum dots occur. This synthesis method is very effective and still used today (Figure 1.6). However, the toxicity of cadmium precursor, dimethylcadmium, and the difficulties of controlling temperature directed researchers into different synthesis methods. Talapin et.al synthesized CdSe / CdS nanoparticles via “greener” method using cadmium acetate as cadmium precursor (Talapin, et al. 2003). Talapin et. al showed that cadmium acetate can be used instead of dimethyl cadmium. Also, Talapin et.al showed that CdSe / CdS / ZnS and CdSe / ZnSe / ZnS core – shell – shell structures can be synthesized by using organometallic route (Talapin, et al. 2004). According to Talapin et. al. both dimethyl cadmium and cadmium acetate can be used in core – shell – shell synthesis. Xu et.al synthesized CdS nanocrystals with organometallic synthesis route using oleic acid as capping agent and made ligand exchange on these nanoparticles.(Yang, et al. 2007) Cao et.al synthesized CdS quantum dots in one pot using octadecene as capping agent (Cao, et al. 2004). By this synthesis method, Cao et.al showed that CdS quantum dots can be fabricated in large scales. Talapin et.al. synthesized CdTe nanoparticles via organometallic synthesis route, using mixture of dodecylamine and trioctylphosphine as capping agents, and obtained highly luminescent CdTe nanoparticles with this method(Talapin, et al. 2001). Peng et.al. synthesized CdS, CdSe and CdTe nanoparticles via organometallic synthesis route using cadmium oxide as cadmium precursor(Peng, et al. 2001). Jiang et.al synthesized CdTeSe alloyed quantum dots via organometallic synthesis route at very high temperature (325 °C), and near IR colored quantum dots

were obtained (Jiang, et al. 2006). Jang et.al. synthesized $\text{CdSe}_x\text{S}_{1-x}$ alloyed quantum dots via organometallic synthesis route and controlled optical properties of $\text{CdSe}_x\text{S}_{1-x}$ quantum dots with changing Se : S ratio (Jang, et.al 2003). Ali et. al. synthesized $\text{CdSe}_x\text{S}_{1-x}$ alloyed nanoparticles by modifying Jang et.al. 's study (Jang, et.al 2003) and obtained white light emitting $\text{CdSe}_x\text{S}_{1-x}$ quantum dots by mixing red, yellow and purple light emitting quantum dots (Pan, et al. 2005).

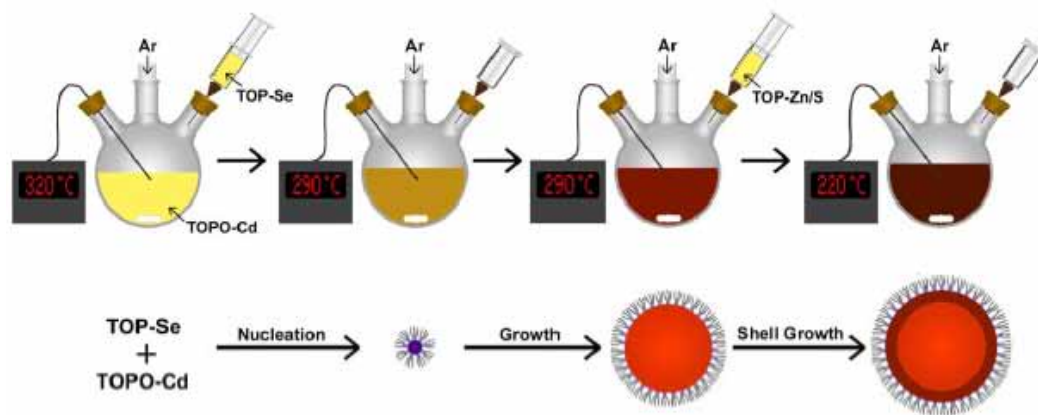


Figure 1.6. Schematic illustration of organometallic synthesis

(Source: Bailey, et.al, 2004)

Pan et.al. derived a new method for synthesizing quantum dots, two – phase synthesis method recently (Pan, et al. 2005). This method allows synthesis of quantum dots in mild conditions, synthesis can be done in low temperature and under atmospheric pressure. Also, autoclaves can be used to control pressure. Basically, Cd precursor (Cadmium Myristate, synthesized from CdO and Myristic Acid) dissolves in oil phase (toluene or heptane) and Se or S precursor dissolves in aqueous phase and reaction occurs at interface of two phases (Figure 1.7). Pan et.al synthesized highly luminescent CdSe / CdS quantum dots via two – phase method in autoclaves with oleic acid as capping agent (Pan, et al. 2005). Pan et.al. synthesized CdS nanoparticles at atmospheric conditions at very low temperature (at 100 °C) corresponding to organometallic synthesis route (at 300 °C) (Pan, et al. 2004). Also Pan et.al synthesized CdS nanoparticles in autoclave at different temperatures varying between 120 °C and 180 °C and developed a seeding technique, to grow bigger nanoparticles by using smaller nanoparticles as starting material (Pan, et al. 2005). Pan et.al synthesized CdS

and CdSe nanoparticles with different Se and S precursors at autoclaves or air conditions at different temperatures and tried to optimize synthesis conditions for two – phase synthesis method (Pan, et al. 2007). Also Pan et.al. synthesized “nano onions” , a core structure surrounded with multiple shells, via two – phase synthesis method (Pan, et al. 2006)

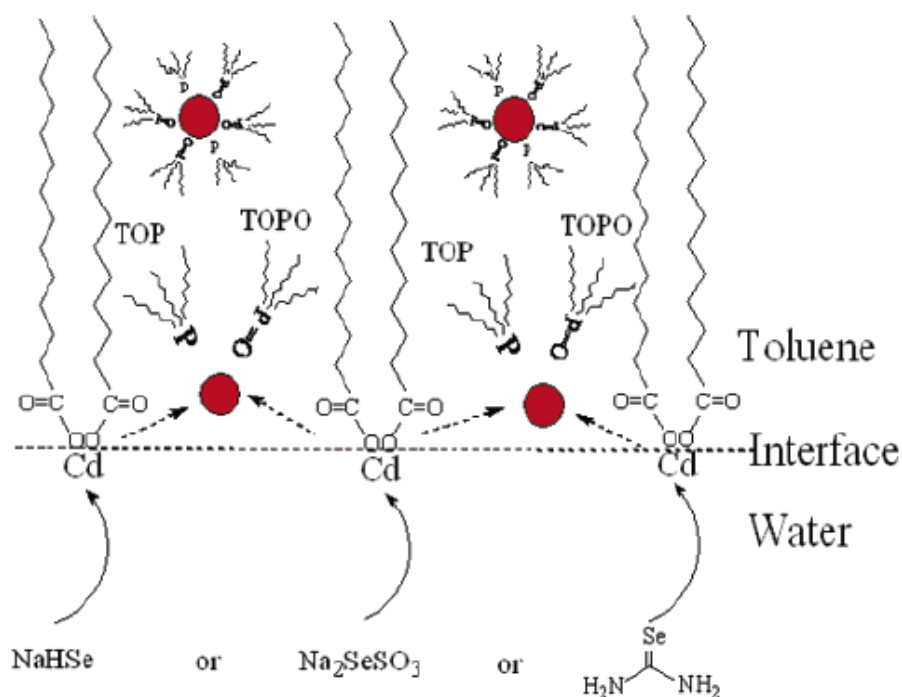


Figure 1.7. A proposed mechanism for formation of CdSe in oil phase
(Source: Pan, et al. 2007)

Also there are studies on synthesis of quantum dots at one step aqueous synthesis. Gaponik et.al. synthesized CdTe nanoparticles in aqueous media by producing $H_2Te(g)$ and bubbling aqueous cadmium solution with H_2Te under N_2 atmosphere and at around $100\ ^\circ C$ with using different capping agents such as 2 – mercaptoethanol, 1 – thioglycerol (Figure 1.8)(Gaponik, et al. 2002). Peng et.al described a one pot synthesis method for CdTe / CdS nanoparticles using thioglycolic acid as capping agent (Peng, et al. 2007). Gu et.al synthesized 3 – mercaptopropionic acid capped CdTe / CdS nanoparticles and obtained highly luminescent by using NaHTe as Te precursor (Zhong, et al. 2008). Gaponik et.al synthesized CdTe nanoparticles with one step aqueous synthesis method using TGA and 3 – MPA as capping agents and compared optical properties of CdTe nanoparticles capped with

TGA and 3 – MPA (Gaponik, et al. 2007). Qian et.al synthesized CdHgTe alloyed nanoparticles surrounded with CdS shell capped with 3 – MPA by one pot synthesis method and obtained near IR colored quantum dots with high quantum yields (Qian, et.al 2007).

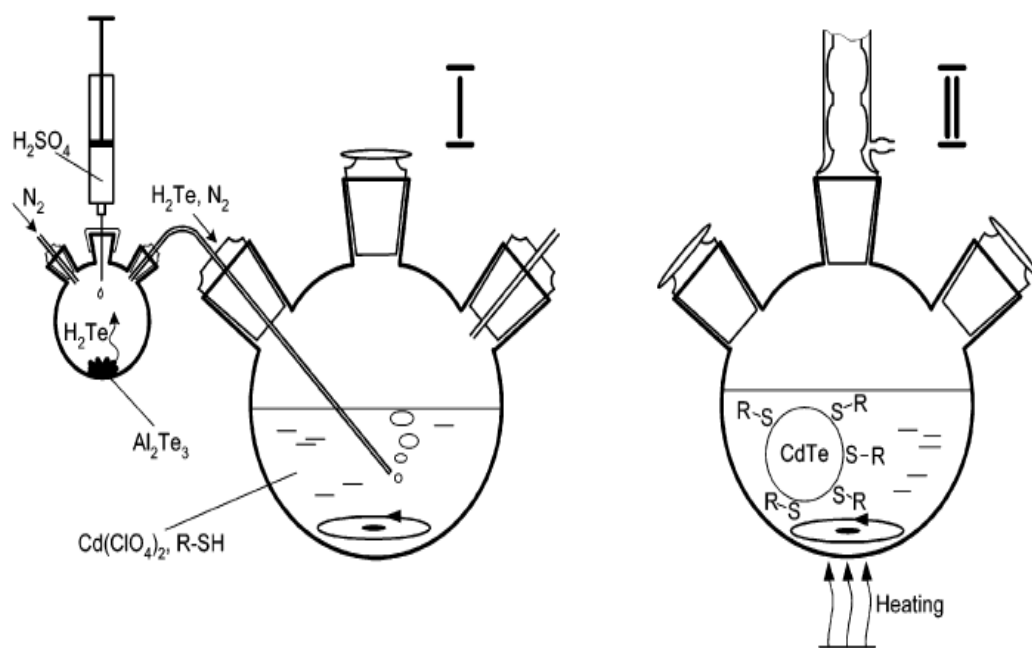


Figure 1.8. Synthesis of CdTe nanoparticles in aqueous media

(Source: Gaponik, et al. 2002)

1.5. Biofunctionalization of Quantum Dots

Bawendi et.al. synthesized quantum dots in TOP and TOPO, soluble in organic solvents such as hexane, heptane, toluene, etc... Oleic acid and octadecene capped quantum dots show same solubility properties as TOPO capped quantum dots. However, for biological applications, quantum dots must be water soluble. In 1997, Alivisatos et.al showed that quantum dots can also be used in biological applications, such as biolabeling, tagging, etc...(Alivisatos, et al. 1998)

There are several methods to make quantum dots water soluble (Figure 1.9). The most studied one of these methods is called the ligand exchange method. Basically, its main purpose is to synthesize oil soluble quantum dots with high quantum yield, and then replace its surfactant with a different surfactant which can be dissolved in water.

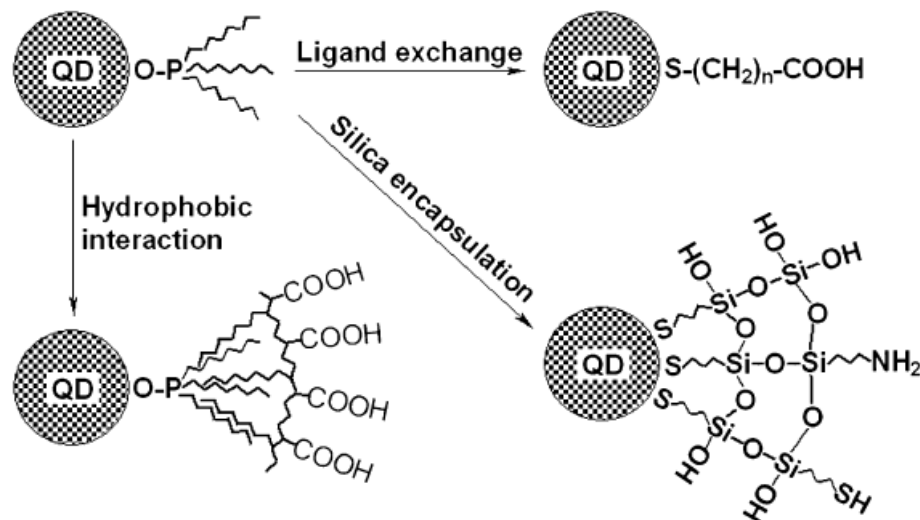


Figure 1.9. Schematic illustration of different methods for making Quantum Dots water soluble (Source: Yu, et al. 2006)

All quantum dots surface chemistries are designed to provide reactive groups such as amine ($-\text{NH}_2$), carboxyl ($-\text{COOH}$) or mercapto ($-\text{SH}$) groups for direct conjugation to biomolecules. Finally, the quantum dots are conjugated to the linker (e.g., avidin, protein A or protein G, or a secondary antibody) by covalent binding passive adsorption, multivalent chelation or by electrostatic interactions.

However, this surface modification may cause defects in crystal structure. Mostly, quantum yield of quantum dot reduces after ligand exchange. To protect the high quantum yield of quantum dots in aqueous media, several studies have been done including micelle formation around the external organic capping layer, (Dubertret, et al. 2002) deposition of additional inorganic coatings such as SiO_2 , (Yang, et al. 2004) and formation of polymer coatings (Wang, et al. 2004). These studies helped quantum dots to maintain their high quantum yield. However, these procedures increased nanoparticles diameter from 2-5 nm to 20-100 nm, which eliminates one of the advantages of using QDs instead of fluorescent dyes and beads, namely, their small size (Pinaud, et al. 2004). Blum et.al. tried to make ligand exchange with long chain alkyl groups with thiol groups (Figure 1.10). They searched effect of alkyn chain length on protection of quantum yield. According to their research, when length of alkyn group increases, quantum dot is surrounded better and less amount of defects occur in crystal structure, as resulting in higher quantum yield is gained (Blum, et al. 2008).

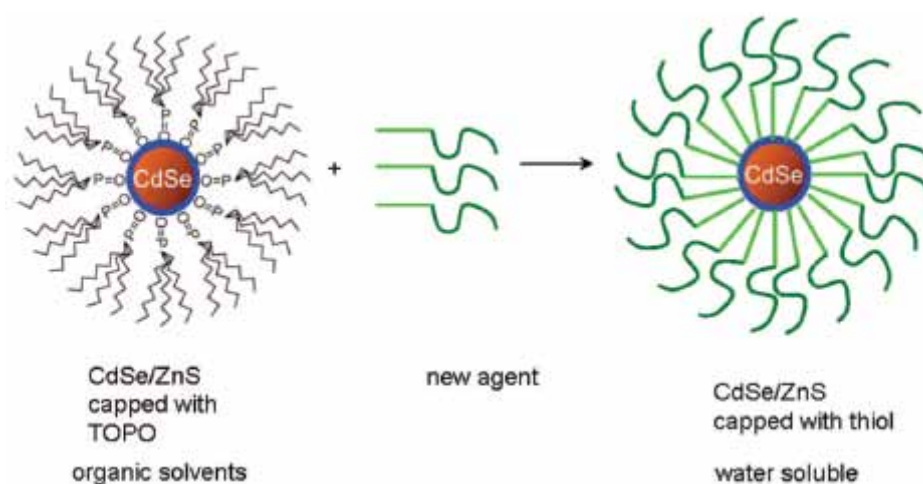


Figure 1.10. Schematic illustration of ligand exchange

(Source: Blum, et al. 2008)

However, Gaponik et.al studied effect of 3 – Mercaptopropionic acid and thioglycolic acid, also known as mercaptoacetic acid, on quantum yield of quantum dots after ligand exchange. Gaponik et.al showed that CdTe nanoparticles have better quantum yield with thioglycolic acid as capping agent than with 3 – Mercaptopropionic acid as capping agent (Gaponik, et al. 2007). Wuister et. al. changed TOPO around CdTe with TGA and 3 – MPA and showed that ligand exchange may cause increase in quantum yield (Wuister, et al. 2003). Zhang et.al. showed that ligand exchange can improve quantum yields of oleic acid capped CdS quantum dots (Zhang, et al. 2008)

Forming a micelle through hydrophobic interaction is another way to obtain water soluble quantum dots. Some phospholipids having both hydrophilic and hydrophobic groups within them can be used to produce water soluble quantum dots. This kind of phospholipids can encapsulate core type quantum dots by forming oil-in-water micelles through hydrophobic interaction between their hydrophobic sides and the surfactants of the quantum dots and provide water-solubility via hydrophilic exterior ends.(Wang, et al. 2004)

Another method to make quantum dots water soluble is silica encapsulation method. By encapsulating quantum dots with a silica layer, quantum dots can also be water soluble and biocompatible. Functional organosilicone molecules containing $-NH_2$ or $-SH$, are incorporated into the shell and provide surface functionalities for biomedical applications. Silica encapsulation method can be considered as a modified

ligand exchange method. Firstly, quantum dots should be solved in a solvent including silane, such as mercaptopropyl(methoxy)silane and by adding base in this solution, surfactant of quantum dot must be replaced with silane groups. With time, methoxysilane silane groups hydrolyze into silanol groups. Heat strengthens silanol – silanol bridges by converting them into siloxane bonds. Surface of quantum dots may be functionalized after this step by adding silane groups including functional groups.(Figure 1.11) However, inserting organosilicones on surface of quantum dots effects quantum yield of quantum dots and decreases the quantum yield. Also coating with silica around quantum dots is relatively complicated when it is compared to other methods. Silica coating needs to be carried out at dilute conditions, which does not permit large quantity fabrication (Gerion, et al. 2001)

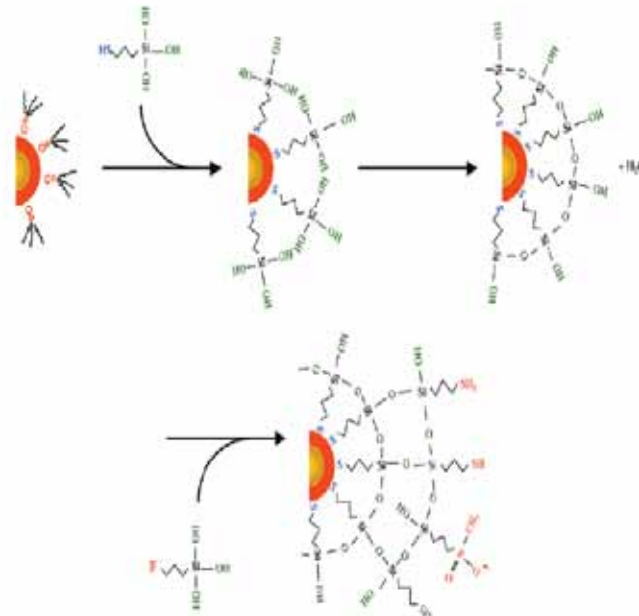


Figure 1.11. Schematic illustration of silica encapsulating
(Source : Gerion, et al. 2001)

Because of disadvantages of these methods mentioned above, researchers tried to synthesize quantum dots directly in aqueous media. However synthesis of CdSe quantum dots does not give good results in terms of quantum yield, generally quantum yields of direct water synthesized CdSe were between %1 and %5 (Bowers, et al. 2005 , Xia, et al. 2007). So, researchers gave their interests into synthesizing different types of quantum dots. Synthesizing CdTe nanoparticles in water results quantum dots with high

quantum yields and covering core CdTe with shell consisting of CdS also results improvements in quantum yield (Peng, et al. 2007). However, high toxicity of CdTe nanoparticles prevents use of these quantum dots in biomedical applications (Cho, et al. 2007). Yet, there are biomedical studies based on CdTe quantum dots and recently scientists has started to use CdTe nanoparticles more efficiently (Fortin, et al. 2005 , Green, et al. 2007).

1.6. Characterization of Quantum Dots

Characterization of quantum dots can be done in many ways. Because of their unique optical properties, UV – VIS Spectrometry and Fluorescence Spectrometry is widely used in characterization of quantum dots. However, to get knowledge about crystal sturcture of quantum dots, some other techniques should be considered. Transmission Electron Microscopy (TEM) and X – Ray Diffractometer (XRD) are generally used for defining crystal structure of quantum dots. Also, Atomic Force Microscopy gives information about crystal structure and monodispersity of quantum dots. For biological applications, toxicity is a very important characteristic property and usually, MTT test is performed to determine toxicity of quantum dots.

1.6.1. Optical Characterization

Optical properties of quantum dots are very important and unique. For that reason optical characterization of quantum dots is very important and should be carried out carefully. UV – Vis and fluorecence spectrometers are used for determining optical properties of quantum dots.

Quantum dots arise in fluorecence and UV – Vis spectrometers as gaussian shaped peaks. These peaks are used to determine size of nanoparticles and growth speed of quantum dots. As quantum dots become bigger, peaks in fluorecence and UV – Vis spectrometers corresponding to quantum dots are red shifted (Figure 1.12).

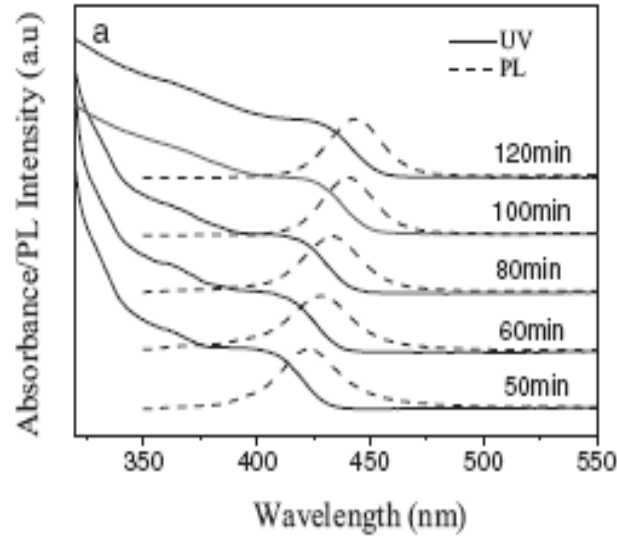


Figure 1.12. Change in fluorescence and UV – Vis Spectra due to CdS quantum dot growth (Source : Pan, et al. 2004)

The width of the peak, typically reported as the full-width-at-half-maximum (FWHM), is generally used to appraise the particle size distribution, in other words, FWHM is used to determine monodispersity of quantum dots. A group of quantum dots consists of individual quantum dots with their own optical and electronic properties and energy levels are dependent upon their sizes. Thus, the emission spectra represent size distributions of individual emissions. The FWHM acts as a statistic that can accurately represent the size distribution.

Stokes shift is the difference between band maxima of fluorescence and absorption spectra of the same electronic transition. This difference is the result of a combination of relaxation into shallow trap states and the size distribution. Stokes shift ($\Delta\nu$) can be found with this formula; $\Delta\nu = \nu_{\text{absorbance}} - \nu_{\text{fluorescence}}$

$$\Delta\nu = \nu_{\text{absorbance}} - \nu_{\text{fluorescence}} \quad (1.5)$$

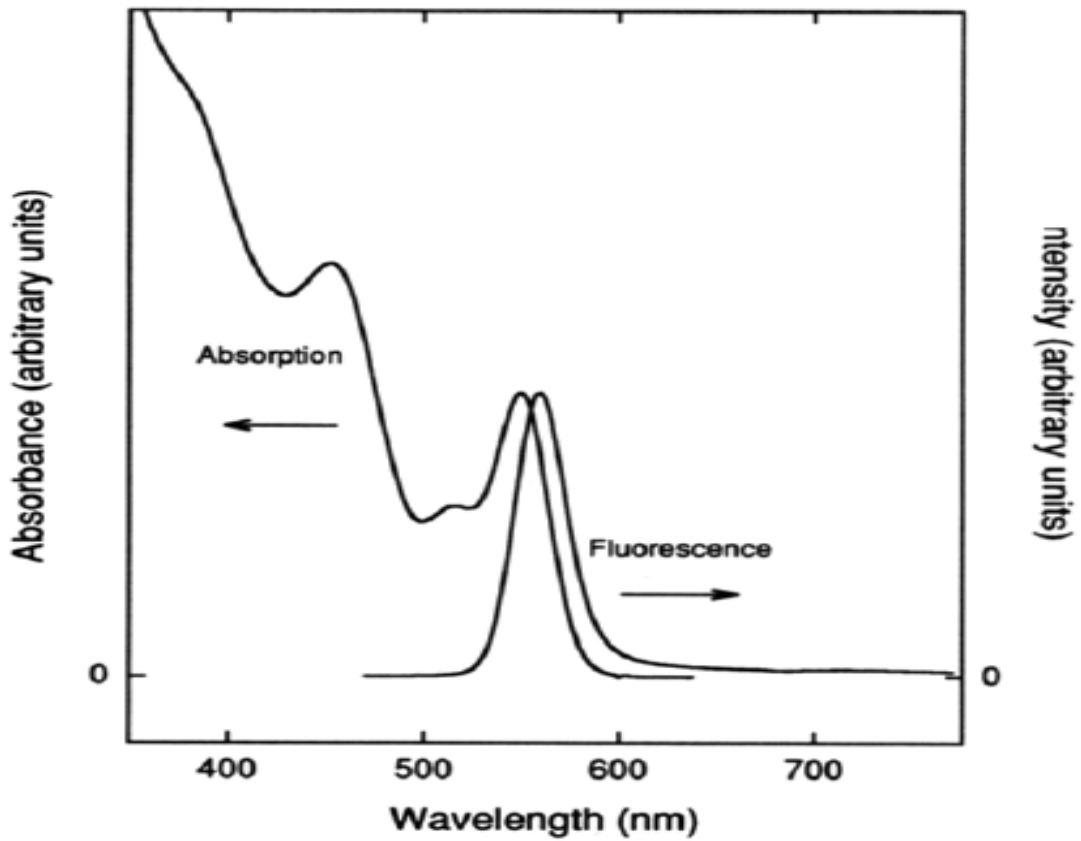


Figure 1.13 Detection of Stokes shift
(Source : Bawendi, et al. 1994)

The fluorescence quantum yield is the ratio of the number of photons emitted to the number of photons absorbed by a fluorescent matter. Experimentally, fluorescence quantum yield of an unknown sample can be determined by measuring fluorescence of unknown substance and fluorescence of a fluorophore of known quantum yield with the same experimental parameters. The quantum yield is then calculated by:

$$F = F_{R,X} \frac{Int \ A_R \ n^2}{Int_R \ A \ n_R^2} \quad (1.6)$$

Where Φ is the quantum yield, Int is the area under the emission peak (on a wavelength scale), A is absorbance at the excitation wavelength, and n is the refractive index of the sample. Φ_R , A_R and n_R are quantum yield, absorbance at the excitation wavelength and refractive index of reference respectively.

Size of quantum dots can be determined by using UV – VIS spectrometer. By finding absorption band edge of quantum dots or effective energy band gap of semiconductor nanoparticle size can be detected. The band gap of nanoparticles is obtained by using the equation

$$(\sigma h\nu)^2 = k(h\nu - E_g) \quad (1.7)$$

σ is molar absorption coefficient of nanoparticles, which is obtained from the measured absorption spectra using Beer- Lambert's law, $h\nu$ is photon energy, k is a proportional factor, and E_g is band gap of nanoparticles with the latter being a function of diameter. A plot of $(\sigma h\nu)^2$ versus $h\nu$ shows an intermediate linear region from which one calculates E_g by data fitting. The diameter of core CdS nanoparticle is then calculated from the following equation

$$E_g = E_{gb} + \frac{h^2}{2d^2} \left(\frac{1}{m_e} + \frac{1}{m_h} \right) - \frac{3.6e^2}{4\pi\epsilon d} \quad (1.8)$$

where E_{gb} is bulk band gap, h is Planck's constant, d_p is diameter of nanoparticle, m_e and m_h are the effective electron and hole masses, respectively, e is the electronic charge, and ϵ is the dielectric constant of nanoparticle. (Ethayaraja, et al. 2003)

For CdS quantum dots from the position of the absorption edge, the average particle size can be determined by using the well-established relation between particle size and absorption onset. The absorption edge (λ_e) is converted into the corresponding particle size by using Henglein's empirical curve that relates the absorption edge (λ_e) to the diameter ($2R$) of the particles. (Narayanan, et al. 2006)

$$2R_{CdS} = 0.1/(0.1338 - 0.0002345\lambda_e) \text{ nm} \quad (1.9)$$

1.6.2. Structural characterization

Structural characterization of semiconductor nanoparticles can be determined by X – Ray Diffractometer (XRD), transmission electron microscopy (TEM), and atomic force microscopy (AFM). By using XRD, crystal structure of nanoparticles can be

determined. Structural analysis of bulk semiconductors are studied for a long time and hkl indexes of these structures are known. By comparing hkl indexes of bulk and nano structures, crystal structure and size of nanoparticle can be determined easily. Also, core and core shell structure can be determined by using XRD by observing peak shifts in XRD spectrum. (Figure 1.14). To find crystal structure of nanoparticles, first of all hkl indices of peaks should be determined and appropriate structure for this crystal structure must be determined (fcc, bcc, etc...). To calculate hkl indices, first of all, spacing between planes in the atomic lattices should be determined by De Bragg’s law;

$$n\lambda = 2d\sin\theta \quad (1.10)$$

where n is the order, λ is the wavelength of X – Rays, d is the spacing between planes in the atomic lattices and θ is the angle between incident andray and scattering plane.

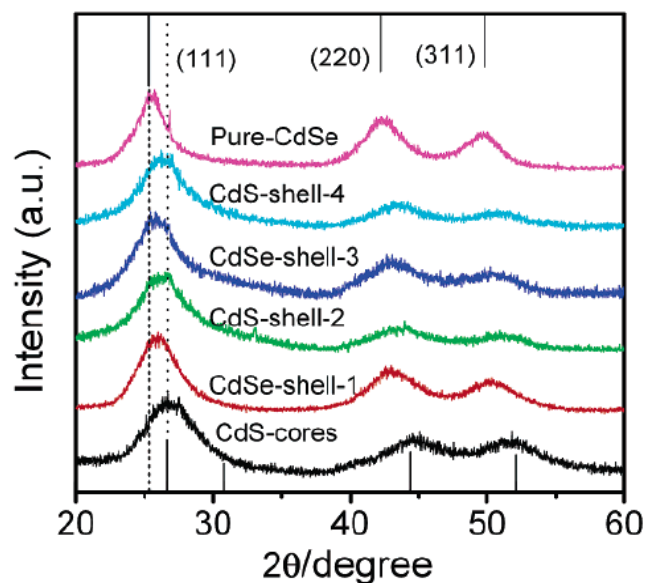


Figure 1.14. XRD patterns of the “nano-onions” with CdS cores capped alternately by CdSe and CdS shells. Vertical lines indicate pure CdSe and CdS reflections (top: zinc blend, CdSe; bottom: zinc blend, CdS).(Source : Pan, et al. 2006)

Also, particle size can be estimated from XRD spectra of nanoparticles. Broadening in XRD peaks occurs due to nano scale of crystal structure and from this broadening nanoparticle size can be determined by Debye – Scherrer equation;

$$D = 0.9\lambda / \beta \cos\theta \quad (1.11)$$

where D is the diameter of the nanocluster, λ the wavelength of the incident X-rays, β is the full-width at the half-maximum, and θ is the diffraction angle.

TEM is the best technique to determine structural characteristics of quantum dots. Size and crystal structure of a quantum dot can be determined exactly by using TEM(Figure 1.15). However, TEM gives information only about a small part of substance.

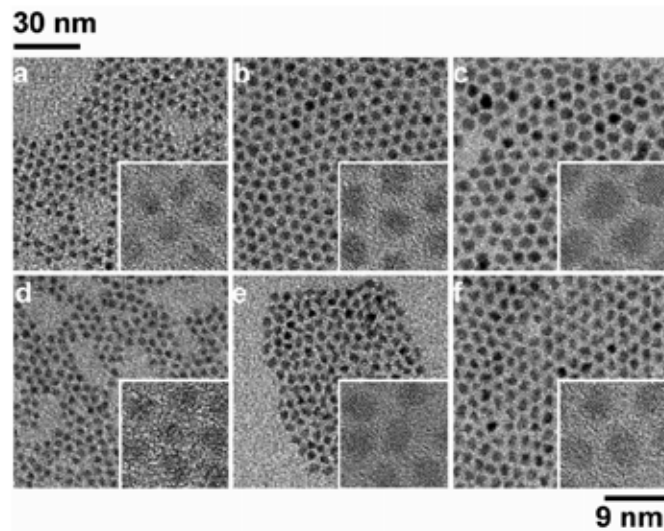


Figure 1.15. TEM image of different sized quantum dots
(Source : Talapin, et al. 2004)

AFM can be used for determining size and monodispersity of nanoparticles (Figure 1.16). However, one disadvantage of AFM is sensitivity of size characterization is limited by tip size. AFM can measure limited size determined by tip of microscope and this leads to errors in analysis.

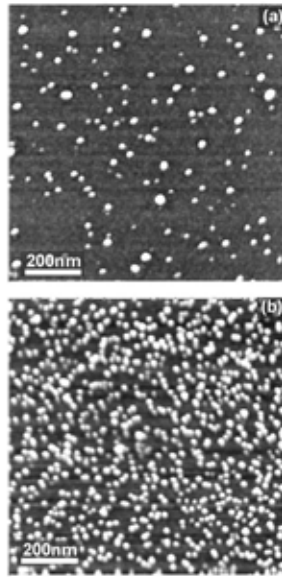


Figure 1.16 AFM image of PbTe quantum dots
(Source : Ferreira, et al. 2001)

1.6.3. MTT Test

MTT Test is a typical laboratory test, a colorometric test, which observes color change in living organisms, cancer cells mostly, due to activity of enzymes that cause reduction of yellow colored 3-(4,5-Dimethylthiazol-2-yl)-2,5-diphenyltetrazolium bromide (MTT) to purple colored formazan. This reduction mechanism happens in mitochondria, it can be said this test observes mitochondrial activity in cells. But also, this test can be used for measuring cytotoxicity of medicinal materials and other toxic materials. Absorption spectrum is used for determining the change in intensity of color. A constant wavelength is chosen around 550 nm and all data is collected due to change in this specific wavelength. Comparing cells injected with toxic material with normal cells without toxic material gives us information about how metabolic activity of cells change due to change in mitochondrial activity.

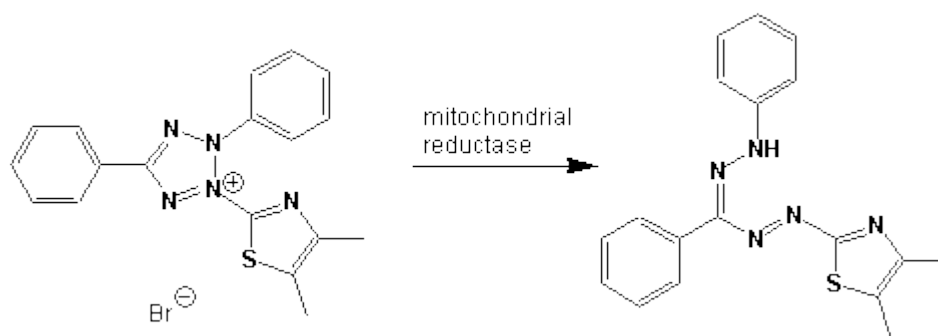


Figure 1.17. MTT reduction scheme

(Source : Mosmann 1983)

1.6.4. Confocal Microscopy

Confocal microscopy is an optical imaging technique which is designed to increase the contrast recording and / or to reconstruct three-dimensional images using a spatial pinhole camera for the elimination of out-of-focus light or flare in samples which are thicker than the focal plane. (Pawley 2006) This technique has become popular in the scientific and industrial communities. Typical applications include life sciences and semiconductor inspection.

Fluorescence confocal microscopy is a type of confocal microscopy which allows to display species with high quantum yields, such as quantum dots and organic dyes, in cells and tissues. If the Stokes shift in these species, organic dye or quantum dot, is large enough, the exciting and fluorescence signals can be totally separated by filters so that only the fluorescence light would reach the detector. With Fluorescence confocal microscopy it is possible to visualize features in living cells and tissues. Confocal fluorescence microscopy is used for obtaining high resolution optical images. Confocal microscopy provides the capacity for direct, noninvasive, serial optical sectioning of intact, thick, living specimens with a minimum of sample preparation as well as a marginal improvement in lateral resolution (Fellers 2007).

Fluorescence confocal microscopy is widely used in bioimaging researches and quantum dots are often used for these bioimaging processes. Anticors can be easily detected in cells with confocal microscopy by binding quantum dots to anticors and inserting them into cell cytoplasm (Figure 1.18).

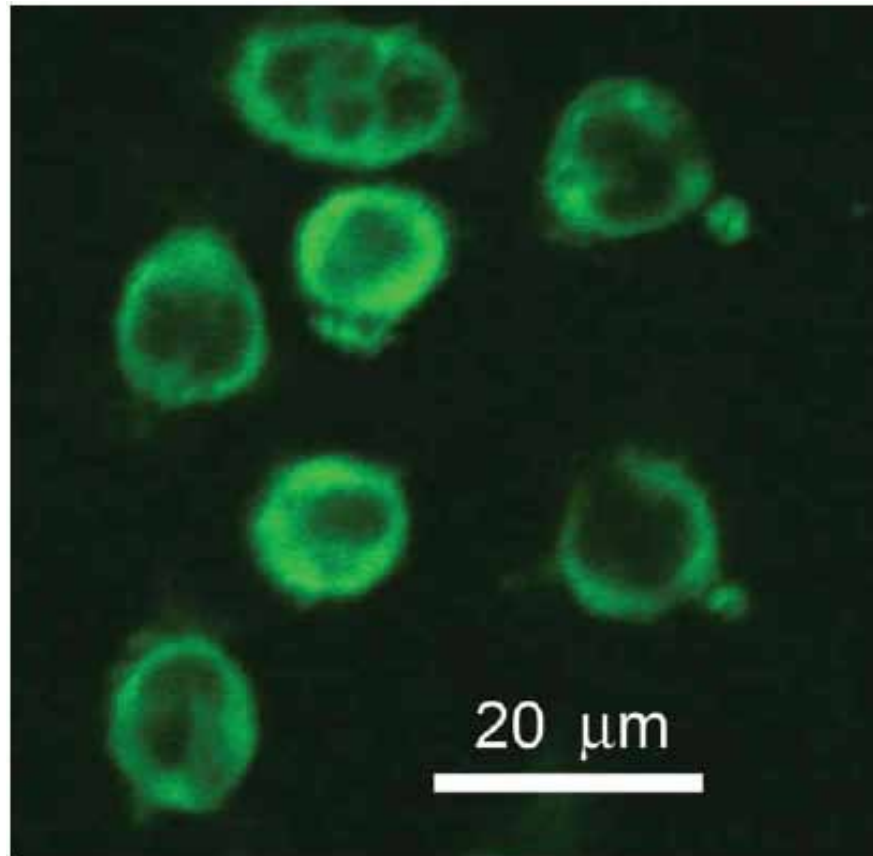


Figure 1.18. Confocal micrograph of peritoneal macrophage from mouse incubated with CdTe QDs-labeled anti-MHC-II (Source : Cunwang et.al., 2007)

1.7. Biological Applications of Quantum Dots

After Bawendi et.al. described simple methods to fabricate monodisperse quantum dots (Bawendi, et al. 1993), researchers have showed great interest on these materials. Because of semiconductor nanocrystal's unique optical properties, quantum dots are used in many industrial and scientific research areas. In early years, quantum dots were successfully synthesized in oil media, such as toluene, heptane, hexane, etc... Because of that, researchers did not think to use quantum dots in biological applications, since materials that are used in biological applications should be soluble in aqueous media. However, after Alivisatos et.al showed that quantum dots can also be water dispersible (Bruchez, et al. 1998). Application area of quantum dots expanded and quantum dots also has been started to be used in biological applications. Including biological applications, quantum dots have been used in many research areas widely

such as light emitting diodes, solar cells, lasers, etc... and there are still many ways to develop and use quantum dots in science and industry.

The fluorescence energy transfer between a donor particle and an acceptor particle at any time that the distance between the donor and the acceptor is smaller than a critical radius, which is called Förster radius, is described as fluorescence resonance energy transfer (FRET). This causes a decreasing in the donor's emission and excited state lifetime, and an increment in the acceptor's emission intensity. FRET is useful for measuring changes in distance, rather than absolute distances and a useful tool for analyzing conformational changes in proteins, monitoring protein interactions. There are studies on quantum dots in FRET technology, when quantum dots are conjugated to biological molecules such as antibodies. (Riegler, et al. 2004, Selvin 2000, Heyduk 2002, Day, et al. 2001, Kagan, et al. 1996)

Quantum dots can also be used in DNA or mRNA tracking. Several groups made studies on quantum dot, which are covered by a surfactant that includes carboxylic groups, conjugated oligonucleotide sequences that bind to DNA or mRNA. When quantum dots compared with organic fluorophores, quantum dots have great advantages over organic fluorophores in terms of optical properties, such as brighter light, greater photostability, etc... However, quantum dot conjugated oligonucleotides are lack in specific binding term, since quantum dots have free carboxylic groups on surface and this leads to nonspecific binding in cells. Because of this nonspecific binding in cells, organic fluorophores are more useful than quantum dot conjugated oligonucleotides. (Pathak, et al. 2001, Gerion, et al. 2002, Xiao, et al. 2004)

Quantum dots may also be used in intra cellular labeling. External labeling of cells with quantum dots is an easy process, however, internal addition of quantum dots has some difficulties. There are some studies on injecting quantum dots in cytoplasm, but none has been considered as exactly successful yet. Some groups used microinjection techniques; however this technique is a very strenuous technique that does not allow high volume analysis. Also there are studies on quantum dots that show uptake of quantum dots into cells via endocytic and non endocytic routes, though these uptakes show only endosomal localizations of quantum dots. There are also studies on injection of amino acid and silica modified quantum dots into cell cytoplasm (Dubertret, et al. 2002, Rieger, et al. 2005, Hanaki, et al. 2003, Jaiswal, et al. 2003, Hasegawa, et al. 2005, Derfus, et al. 2004)

Quantum dots can serve as detectors for pathogens and toxins. These nanocrystals can be used for defining pathogens and toxins properties, including virulence. There are studies on this subject which are resulted in good outcomes, including *Cryptosporidium parvum*, *Giardia lamblia*, *Escherichia coli* 0157:H7 , *Salmonella Typhi*, *Listeria monocytogenes*, *C. parvum* and *G. Lamblia*. However, it is shown that quantum dot based assay is not as sensitive as elisa based tests.(Lee, et al. 2004, Zhu, et al. 2004, Yang, et al. 2006, Tully, et al. 2006)

Different from cell imaging, also qauntum dots are used for whole body imaging, however, there are some difficulties in whole animal body imaging and there is a little work on this subject. The main difficulty is toxicity of quantum dots on both animals and human. Also autofluorescence of tissues is another difficulty in fluorescence tissue monitoring. Tissue autofluorescence minimizes in near infrared region (700 – 1000 nm) and fabricating quantum dots that emit light in near infra red region can solve this problem. However, toxicity of quantum dots is a problem that should be solved completely to use quantum dots in tissue imaging safely. (Lim, et al. 2003, Frangioni 2003)

CHAPTER 2

DEVELOPMENT OF CdTe / CdS QUANTUM DOTS

Recently, CdTe nanocrystals have been used in biological applications by many research groups. CdTe nanoparticles are preferred because of easy fabrication and high quantum yield in aqueous media (around 40%) (Gaponik, et al.). By coating CdTe core with CdS shell, it is possible to obtain even higher quantum yields (around 70%) (Zhong, et al.). In this chapter synthesis and characterization of CdTe / CdS quantum dots are discussed.

2.1. Experimental

2.1.1. Synthesis of NaHTe as Te precursor

Te powder (0.4 mmol) and NaBH₄ (1 mmol) were put into 50 ml reaction flask and it was purged with N₂. Then 10 ml of distilled water added to the reaction flask and the system was heated at 80 °C for 30 minutes under N₂ atmosphere to obtain a solution with a purple color. No other purification techniques were performed. In all experiments, freshly synthesized NaHTe was used. Excess NaHTe was not stored for other experiments to prevent oxidation of precursor (Zhong, et al. 2008). The reaction considered to be as below;



2.1.2. Synthesis of CdTe core nanoparticles

A modified method from literature was used (Zhong, et al. 2008). CdCl₂ (0.2 mmol) and 3 – Mercaptopropionic acid (3 - MPA) (0.4 mmol) was dissolved in distilled water (40 ml) and pH was adjusted to 12 by adding 1.0 M NaOH solution. Then the solution transferred into a two – necked flask and bubbled with N₂ to purge oxygen in the medium. While bubbling solution, temperature set to 100 °C and kept

constant during reaction. Then 1 ml of freshly synthesized NaHTe was added to the solution and the reaction started. After 10 minutes, the color of solution was green under UV – irradiation and green light was observed. Then the reaction is stopped by lowering temperature to room temperature.

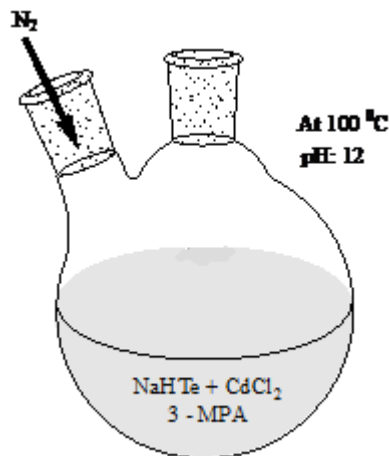


Figure 2.1. Schematic Illustration of Synthesis of CdTe

2.1.3. Synthesis of CdTe / CdS core – shell nanoparticles

0.08 mmol of Thiourea (Figure 2.2) solution was added to the CdTe nanoparticle solution at 100 °C under N₂ atmosphere. After 15 minutes core – shell structure started to grow. Aliquots of sample were taken at different time intervals and their optical properties were monitored by using UV – Vis and fluorescence spectra. The reaction was stopped at desired time by cooling solution. Formed nanoparticles were precipitated by adding ethanol on solution. Precipitation procedure was repeated several times to remove impurities.(Zhong, et al. 2008)

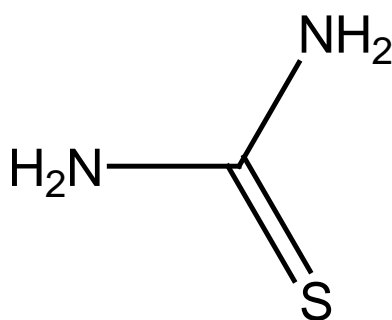


Figure 2.2. Structure of Thiourea

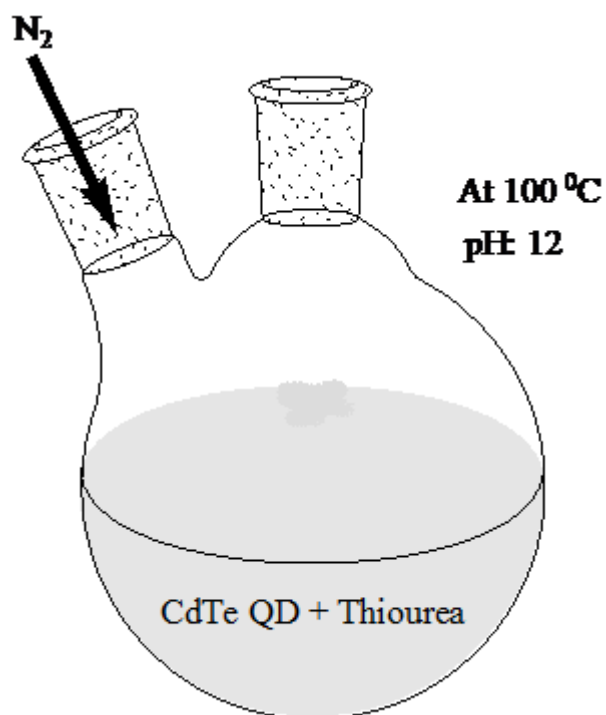


Figure 2.3. Schematic illustration of Synthesis of CdTe / CdS core – shell quantum dots

2.2. Characterization

2.2.1. Optical Characterization

Optical characterization of quantum dots was done by using UV – Vis and fluorescence spectroscopy. Fluorescence and UV – Vis Spectra are very important characterization tools for CdTe / CdS quantum dots and used widely in quantum dot production to monitor how reaction proceeds

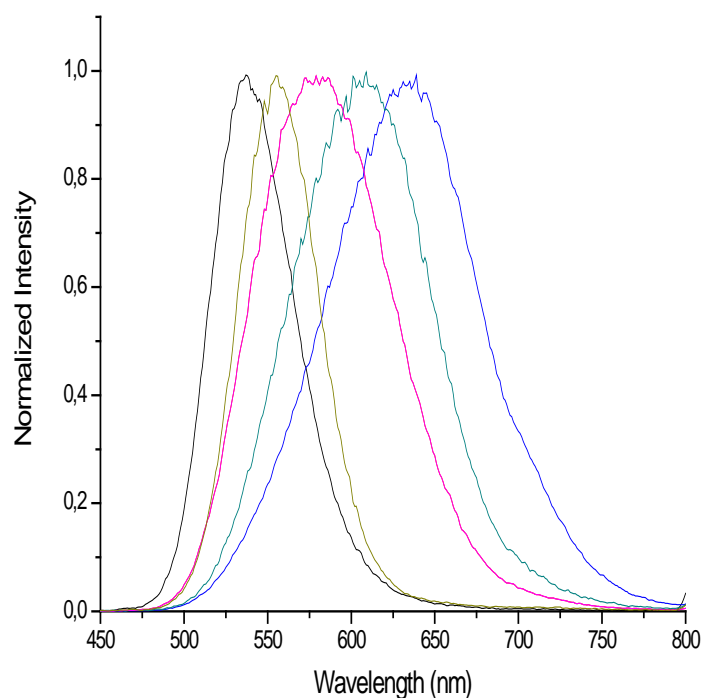


Figure 2.4. Normalized fluorescence spectrum of CdTe / CdS nanoparticles synthesized at different time intervals.

Figure 2.4 shows time dependent growth of CdTe / CdS nanoparticles. Growth of CdTe / CdS nanoparticles started at first 30 minutes and continued for 6 hours. However, particles may grow bigger in size if reaction was allowed to continue. In Figure 2.4, the growth of CdTe / CdS nanocrystals can be monitored by the red shift of spectrum. The spectra were shifted from 540 nm to 630 nm. Within this range, the color of quantum dot was varied from green to red. In Figure 2.5, luminescence image of CdTe / CdS nanoparticles are shown. At 540 nm, quantum dots emit green light and when the size of particles become bigger, the particles emit at higher wavelengths. At 630 nm, the color of CdTe nanoparticles was close to red.



Figure 2.5. Luminescence image of CdTe / CdS nanoparticles under UV lamp

The growth of CdTe / CdS nanoparticles is time dependent. At first, the growth rate of the particles is faster but when the particles become larger, the growth rate slows down. In Figure 2.6, the growth of CdTe / CdS nanoparticles is shown.

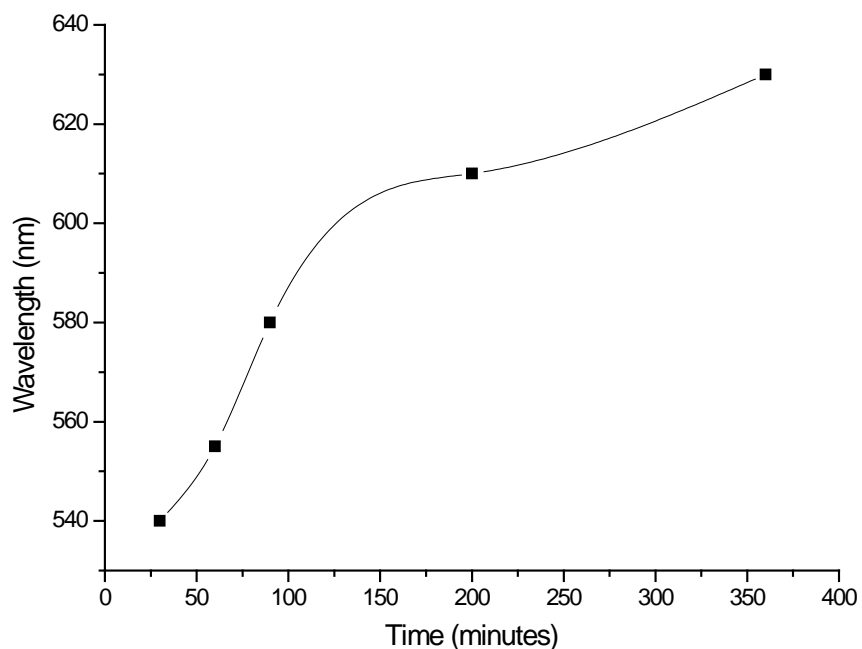


Figure 2.6. Temporal evolution of fluorescence peaks of CdTe / CdS nanoparticles

The growth of CdTe / CdS nanoparticles can also be observed by using UV – vis spectroscopy. (Figure 2.7) A steady shift of spectra to higher wavelength is obvious; indicating an increase in the size of CdTe / CdS nanoparticles .

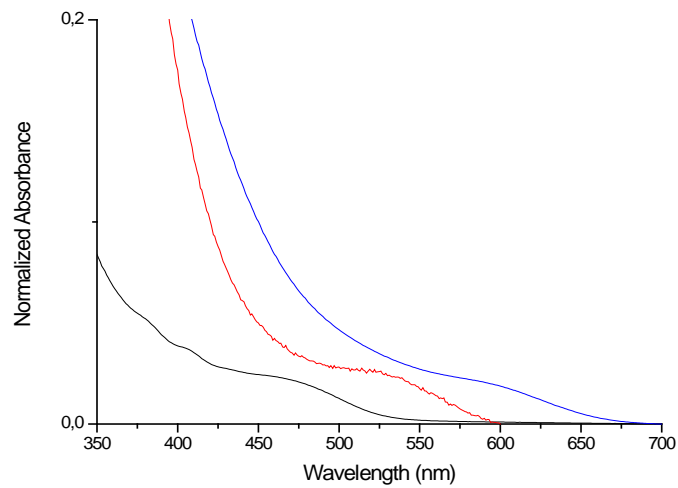


Figure 2.7 UV – Vis spectra of green, yellow and red emitting CdTe / CdS nanoparticles

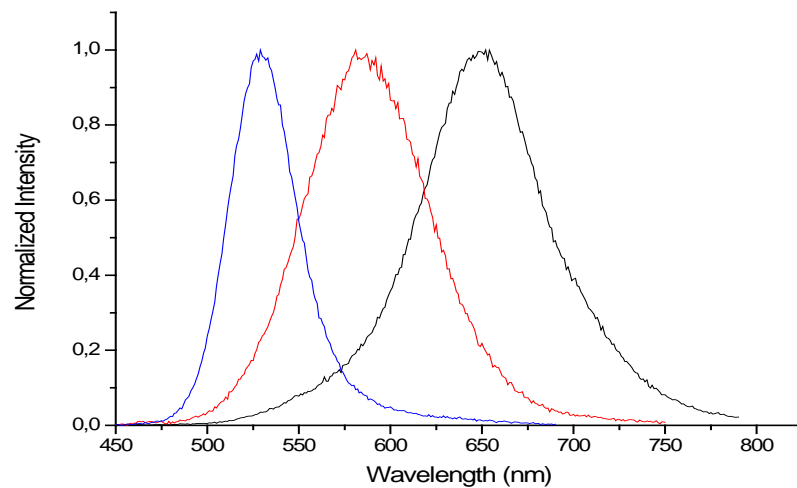


Figure 2.8. Fluorescence spectra of green, yellow and red emitting CdTe / CdS nanoparticles

The bandwidths of CdTe / CdS whose emission peaks are at different wavelengths can be calculated by measuring full width at half maximum (FWHM).

FWHM of CdTe / CdS nanoparticles become broader when particles get bigger. Stokes shift can be calculated from difference of maxima of emission and excitation peak wavelengths Stokes shifts slightly increases with change in particle size, remains constant after a certain size (Table 2.1). The FWHM increased for green CdTe / CdS nanoparticles. However at longer wavelengths, the FWHM is substantially larger, that is reaching to approximately 100 nm. Energy band gap (E_g) of nanoparticles can be determined from UV – Vis spectrum of nanoparticle by cutting wavelength axis by extrapolating first excitation peak in spectrum. E_g of nanoparticles varied from 532 nm to 650 nm (Table 2.1)

Quantum yield (QY) of this nanoparticles are calculated by using Rhodamine 6G in water (QY: %95) as reference. QY of nanoparticles vary between 8% and 35%, the highest QY is observed for yellow color emitting CdTe / CdS nanoparticles (at 580 nm). QY of CdTe / CdS nanoparticles synthesized in this study is exhibiting an increase followed by a decrease and at around 700 nm, QY is below 1%. Table 2.1 reviews photophysical properties of CdTe / CdS nanoparticles.

Table 2.1. Photophysical Properties of CdTe / CdS nanoparticles

Sample Name	$\lambda_{\text{Absorption}}$ (nm)	$\lambda_{\text{Fluorescence}}$ (nm)	Stokes Shift (nm)	FWHM (nm)	QY (%)	E_g	
						(nm)	(eV)
CdTe / CdS 1	485	540	55	55	8	534	2.3
CdTe / CdS 2	500	555	55	56	21	550	2.2
CdTe / CdS 3	520	580	60	96	32	596	2.1
CdTe / CdS 4	550	610	60	97	28	623	2
CdTe / CdS 5	580	630	60	100	6	650	1.9
CdTe / CdS 6	---	700	---	170	1 <	---	---

2.2.2. Structural Characterization:

Quantum dot synthesis can be considered as crystal growth in nano scale. TEM and AFM are important microscopy techniques for structural analysis of quantum dot. In addition to these techniques, XRD is a very useful technique to determine the crystal structure of quantum dots. In Figure 2.9, XRD analysis of CdTe / CdS nanoparticles is shown. Crystal structure of CdTe / CdS nanoparticles was estimated to be face centered cubic by the diffraction angles (2θ) with those of bulk cubic CdTe and CdS from literature (Zhong, et al. 2008, Pan, et al. 2007). The narrowing in XRD peaks shows that the size of particles increases with time, and this result is in consistent with the UV – Vis and fluorescence spectroscopies. From Debye – Scherrer equation (Equation 1.11), size of nanoparticles were found to be varied between 5.4 nm and 9.3 nm (Table 2.2)

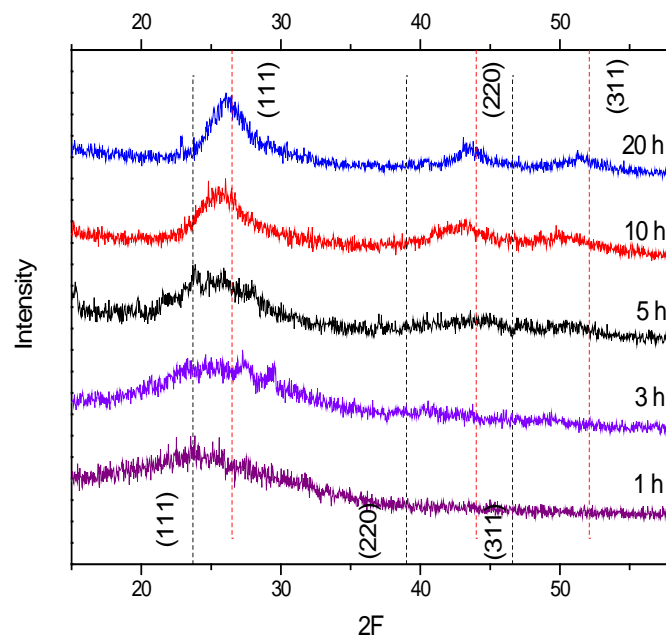


Figure 2.9. XRD spectra of yellow and red emitting CdTe / CdS nanoparticles, the lines representing red dots show hkl indices of face centered cubic bulk CdTe (bottom), the lines with black dots hkl indices exhibits face centered cubic bulk CdS (top)

Table 2.2. Size Analysis of CdTe / CdS Nanoparticles with XRD

Reaction Time (hour)	Size (nm)
1	4.7
3	5.2
5	5.4
10	8.7
20	9.3

However, hydrodynamic size of nanoparticles differs from the crystal size calculated by XRD. Hydrodynamic radius of nanoparticles is bigger than the crystal size of nanoparticles that are calculated by XRD or observed by TEM. Figure 2.10 and Figure 2.11 show Dynamic Light Scattering studies of yellow and red CdTe / CdS nanoparticles. The hydrodynamic radius of nanoparticles is bigger than the crystal size of nanoparticles that are calculated by XRD (Table 2.3). This difference is due to hydration layer of water molecules.

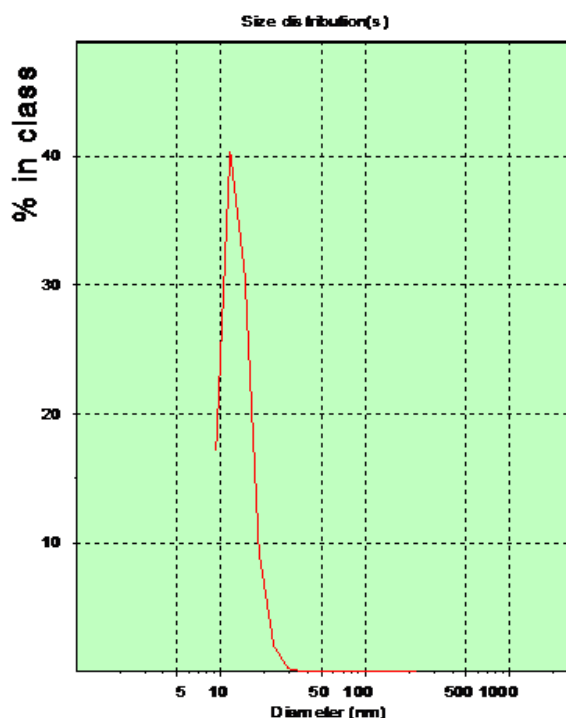


Figure 2.10. DLS analysis of yellow CdTe / CdS nanocrystals

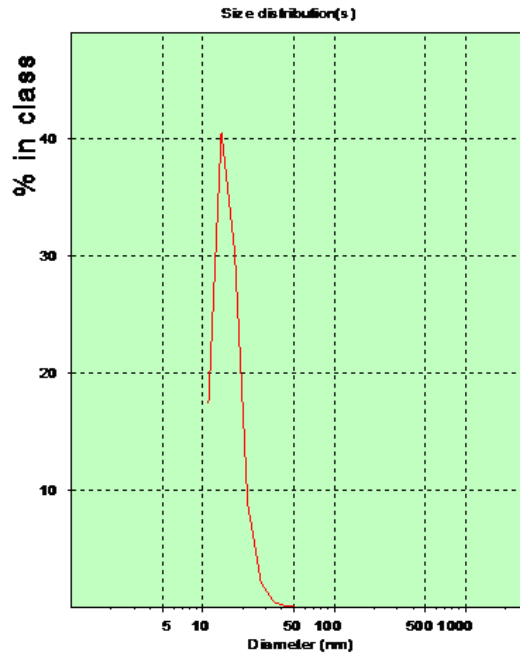


Figure 2.11. DLS analysis of yellow CdTe / CdS nanocrystals

The size of nanoparticles can also be determined from UV – Vis spectroscopy by using equation 1.7. From literature, E_{gb} of CdTe is found to be 1.49 eV, m_e of CdTe is $0.098 m_0$, m_h of CdTe is $0.11 m_0$ and ϵ is $10.3 \epsilon_0$ (m_0 is free electron mass and ϵ_0 is vacuum dielectric constant) (Strzalkowski, et al. 1976, Banerjee 2000, El Moussaouy, et al. 2006). By inserting these values into the Equation 1.8, the second order equation below is determined,

$$\frac{1878}{\lambda} = 2.39 + 83 \frac{1}{d^2} - 0.806 \frac{1}{d} \quad (2.1)$$

where λ is first exciton peak cutting through wavelength axis in absorption spectrum and d is diameter of nanoparticle. By solving this 2nd order equation, the equation below is determined,

$$\frac{1}{d} = 0.0048 + \sqrt{\frac{22.63}{\lambda} - 0.029} \quad (2.2)$$

However, the results determined from Equation 2.2 is quite different from the results determined from XRD.(Table 2.3)

Table 2.3. Size determination of CdTe / CdS nanoparticles from XRD, UV – Vis spectroscopy and DLS

Sample Name	Size of CdTe / CdS nanoparticle from XRD (nm)	Size of CdTe / CdS nanoparticle from UV – vis (nm)	Hydrodynamic size of CdTe / CdS nanoparticle from DLS (nm)
Green CdTe / CdS nanoparticles	4.7	8.3	---
Yellow CdTe / CdS nanoparticles	5.2	10.1	13.1
Red CdTe / CdS nanoparticles	5.4	13.2	15.7

Table 2.4 summaries amount of Cd and Te in 1 ppm solution of different sized CdTe / CdS nanoparticles from ICP – MS analysis. Amount of Cd increases with larger size of nanoparticle, however amount of Te is not correlated with size.

Table 2.4 ICP – MS analysis of CdTe / CdS nanoparticles

Sample Name	Cd (ppb)	Te (ppb)
CdTe / CdS 1	112.7	33.9
CdTe / CdS 2	310.6	121.7
CdTe / CdS 3	687.1	56.2

2.2.3. Biological Characterization

2.2.3.1. MTT Studies

2.2.3.1.1. Preparation of Cell Culture

Human Prostate Cancer (PC3) and MCF7 were used for biological characterization of the nano particles. PC3 cell line was kindly provided by Associate

Professor Kemal Sami Korkmaz (Ege University, Engineering Faculty, Department of Bioengineering). Cells were maintained in Dulbecco's modified Eagle's medium (DMEM) containing 5% fetal bovine serum (FBS) (BIO-IND), 50µg/ml gentamicin sulfate, incubated at 37°C in the dark with 5% CO₂ and 95% humidification and passaged when they reached 80-85% confluency.

2.2.3.1.2. Treatment of Cultured Cells with Compounds and Cell Viability Assay

To investigate the cytotoxic activity of the extracts, 95µl of cell suspension was inoculated into 96-well microculture plates at 1×10^4 cells density per well in culture media containing FBS, gentamicin sulfate. Compounds were dissolved in DMEM, filter sterilized, diluted at the appropriate concentrations with the culture medium. Dilutions of compounds were freshly prepared before each experiment. After 24h cultivation for cell attachment, the nanoparticles were added at final concentration 0,0001 µg/ml, 0,001µg/ml, 0,01µg/ml, 0,1 µg/ml 1 µg/ml, 2,5 µg/ml, 5 µg/ml, 10 µg/ml, 25 µg/ml, 50µg/ml, 100µg/ml for triplicate assay. Cells were treated with the nanoparticles for 24 hours and 48 hours, and cytotoxic effects were determined by tetrazolium (3-{4,5-dimethylthiazol-2-yl}-2,5-diphenyl tetrazolium bromide) (Sigma Chemical Co.) based on colorimetric assay. This method depends on the cleavage of tetrazolium salt to purple formazan crystals by mitochondrial enzymes of metabolically active cells (Ciapetti, et al. 1993). Briefly; 4 hours before the end of each incubation period, medium of the cells was removed and wells were washed by pre-warmed phosphate-buffered saline (PBS) to remove any trace of the nanoparticles and to prevent colour interference while optical density determination. MTT stock solution (5mg/ml) was diluted at 1:10 ratio into complete culture media, 100µl of MTT dilution was added into each well and incubated. After 3,5 hours plates were centrifuged at 1800 rpm for 10 minute at room temperatures to avoid accidental removal of formazan crystals. Crystals were dissolved with 100µl DMSO. The absorbance was determined at 540nm. Results were represented as percentage viability and calculated by the following formula:

$$\% \text{ viability} = 100 - [(OD_s - OD_b / OD_c - OD_b) \times 100]$$

OD_b indicated the optical density of blank, OD_s indicated the optical density of sample and OD_c indicated the optical density of control.

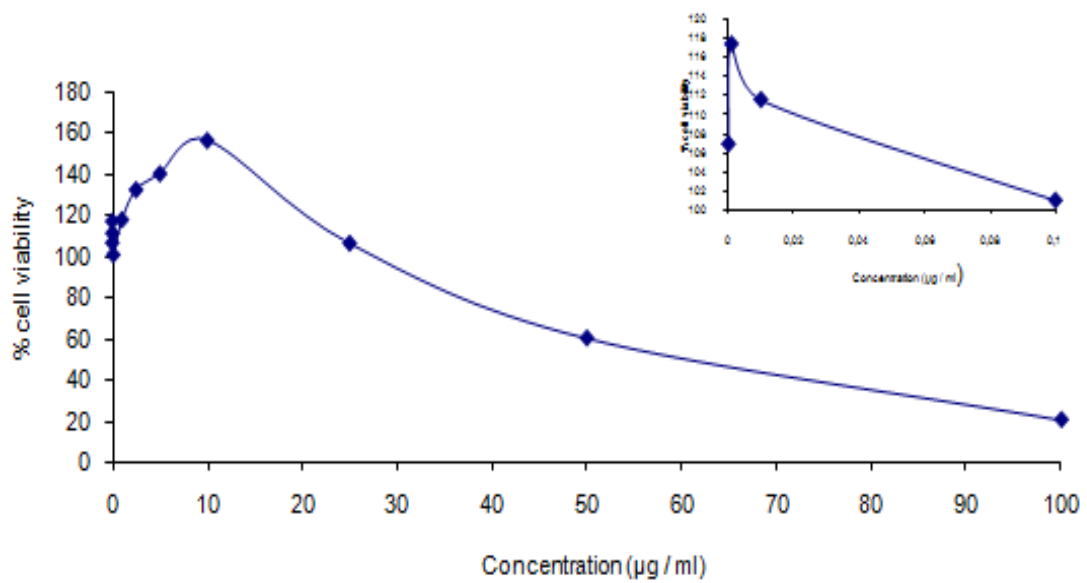


Figure 2.12. MTT results for green CdTe / CdS quantum dots in MCF7 cells for 1 day

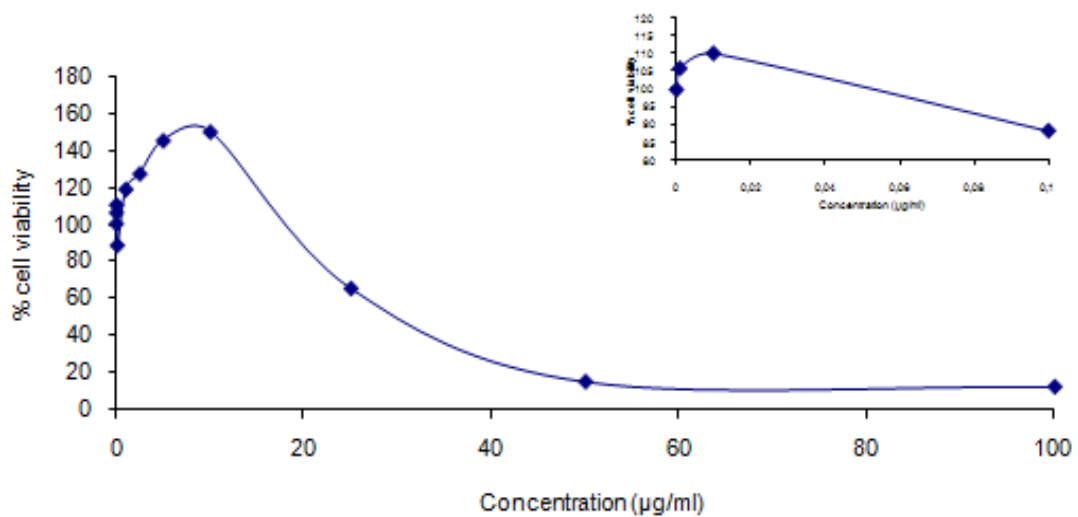


Figure 2.13. MTT results for green CdTe / CdS quantum dots in MCF7 cells for 2 days

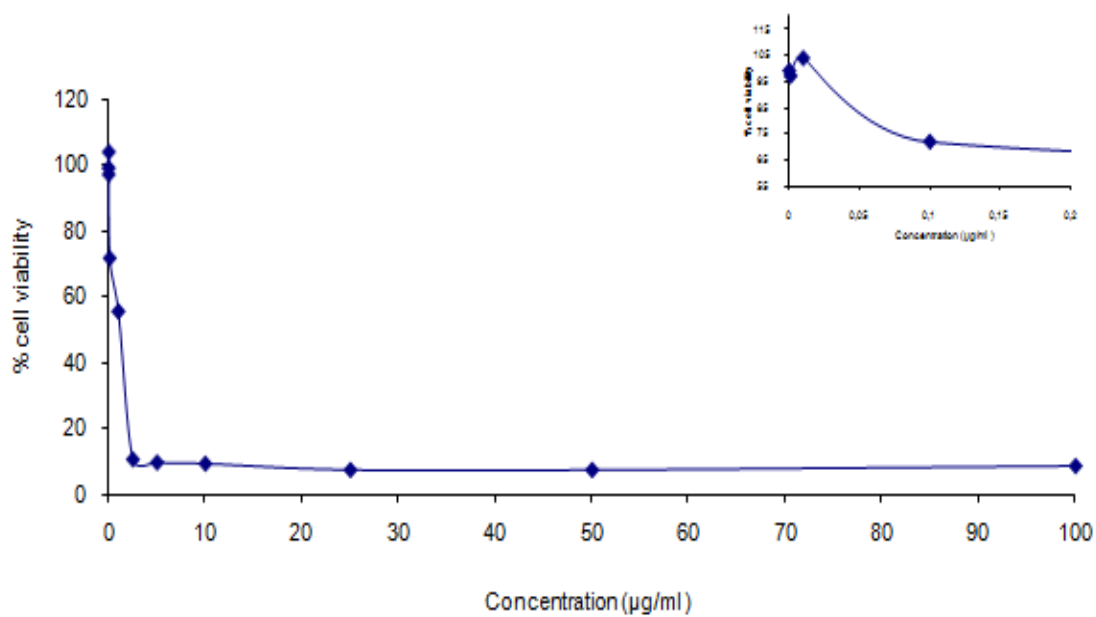


Figure 2.14. MTT results for green CdTe / CdS quantum dots in PC3 cells for 1 day

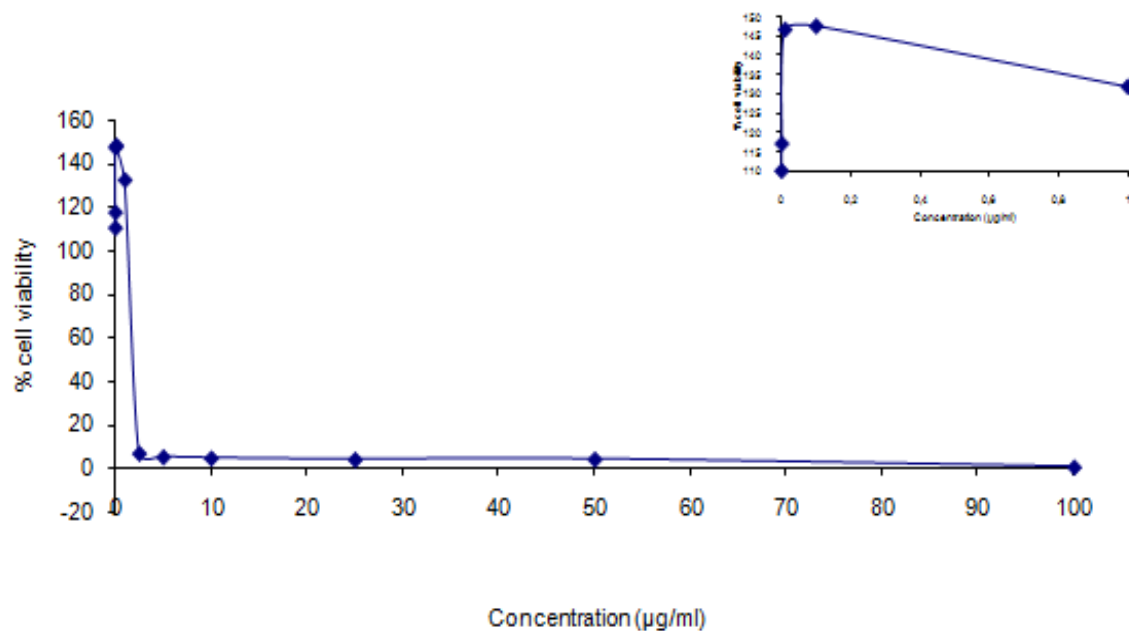


Figure 2.15. MTT results for green CdTe / CdS quantum dots in PC3 cells for 2 days

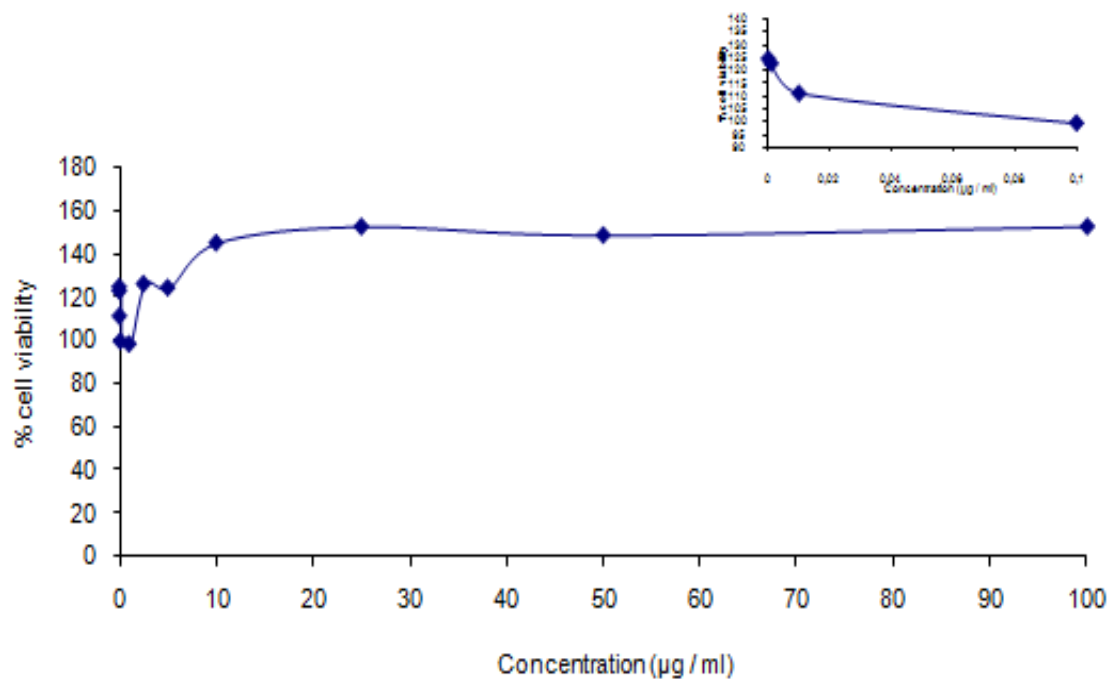


Figure 2.16 MTT results for yellow CdTe / CdS quantum dots in MCF7 cells for 1 day

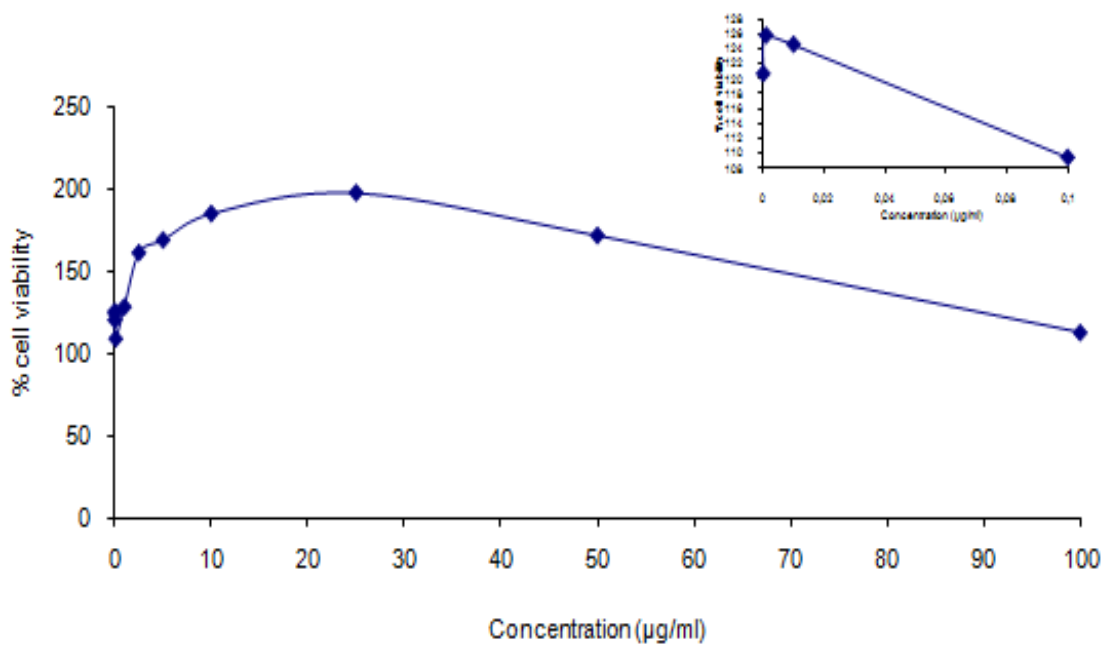


Figure 2.17 MTT results for yellow CdTe / CdS quantum dots in MCF7 cells for 2 days

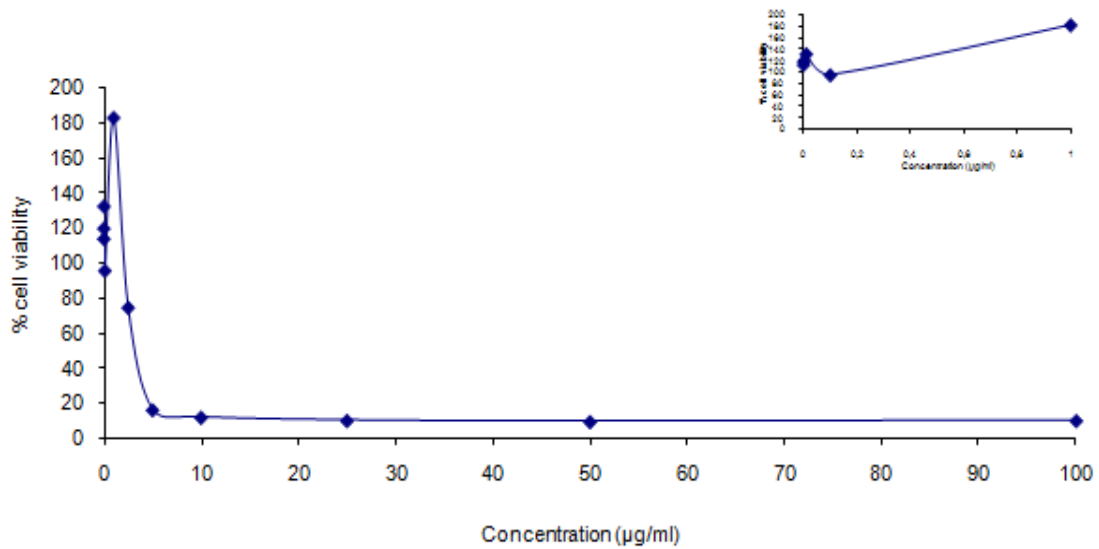


Figure 2.18. MTT results for yellow CdTe / CdS quantum dots in PC3 cells for 1 day

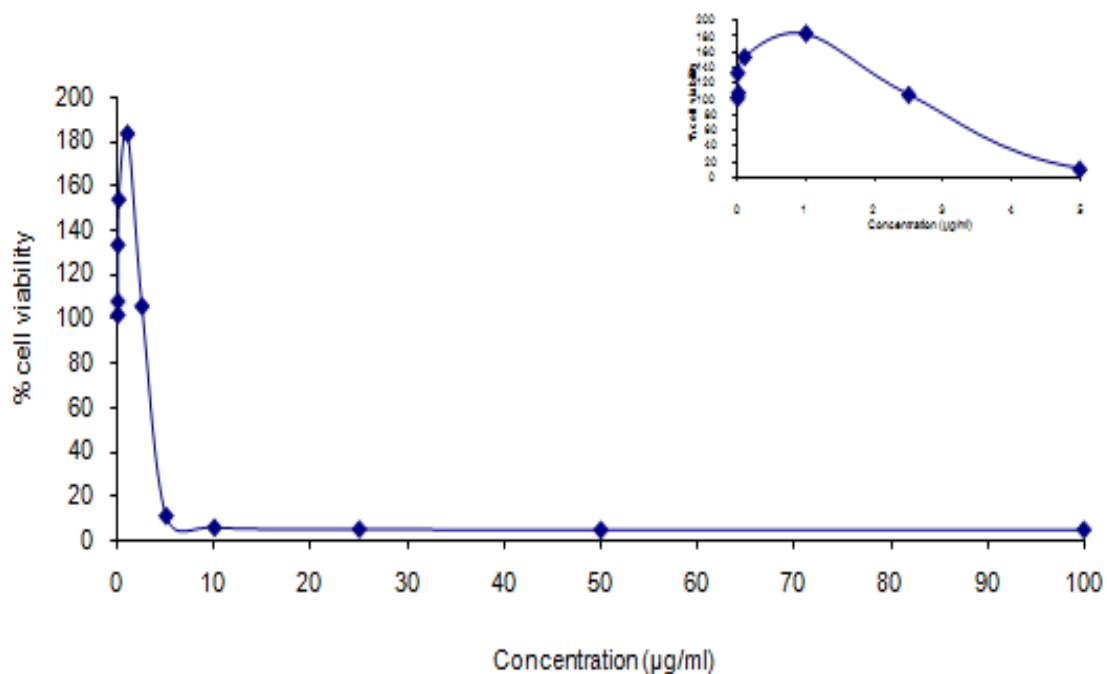


Figure 2.19. MTT results for yellow CdTe / CdS quantum dots in PC3 cells for 2 days

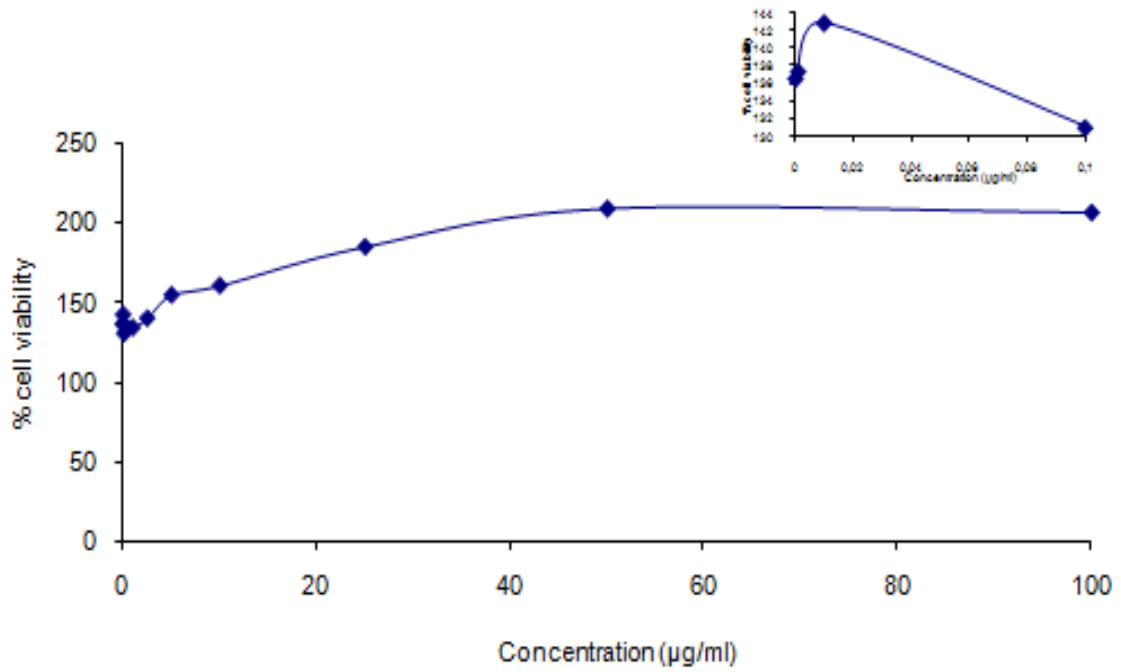


Figure 2.20. MTT results for red CdTe / CdS quantum dots in MCF7 cells for 1 day

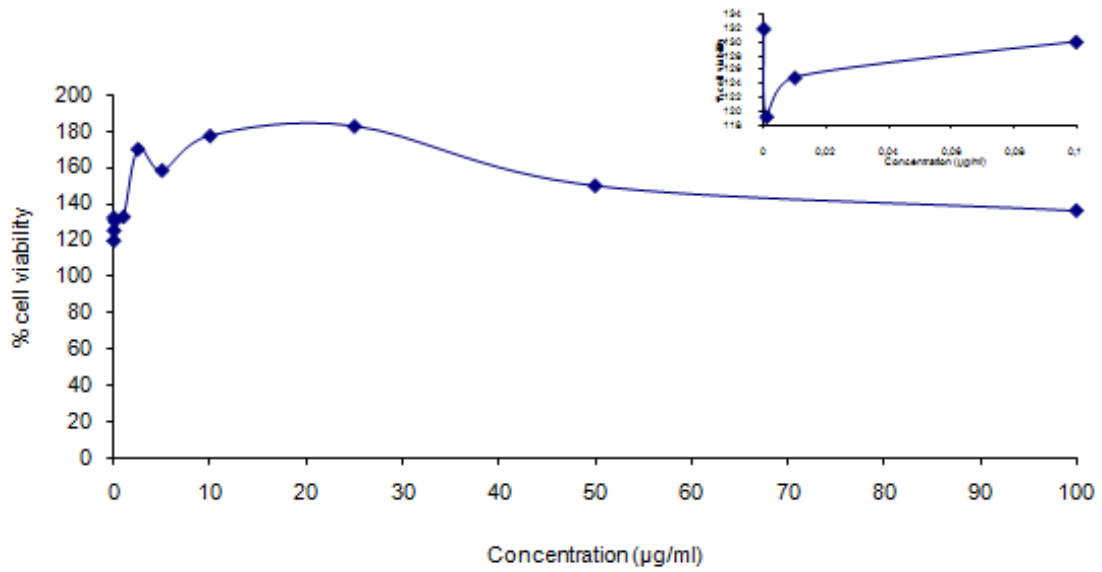


Figure 2.21. MTT results for red CdTe / CdS quantum dots in MCF7 cells for 2 days

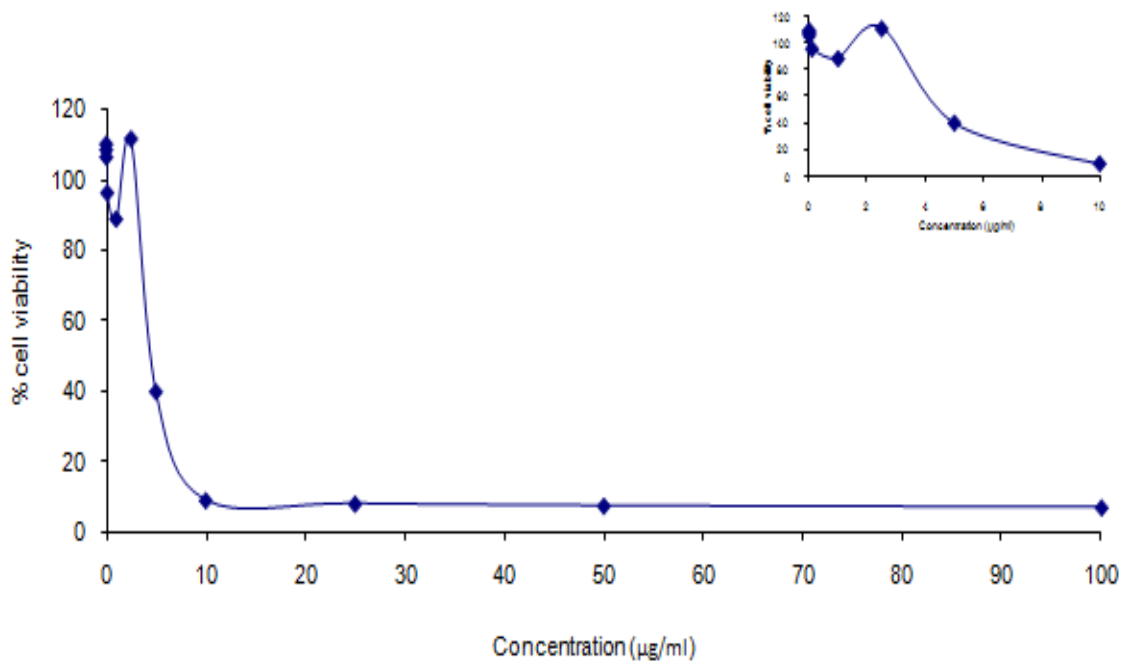


Figure 2.22.MTT results for red CdTe / CdS quantum dots in PC3 cells for 1 day

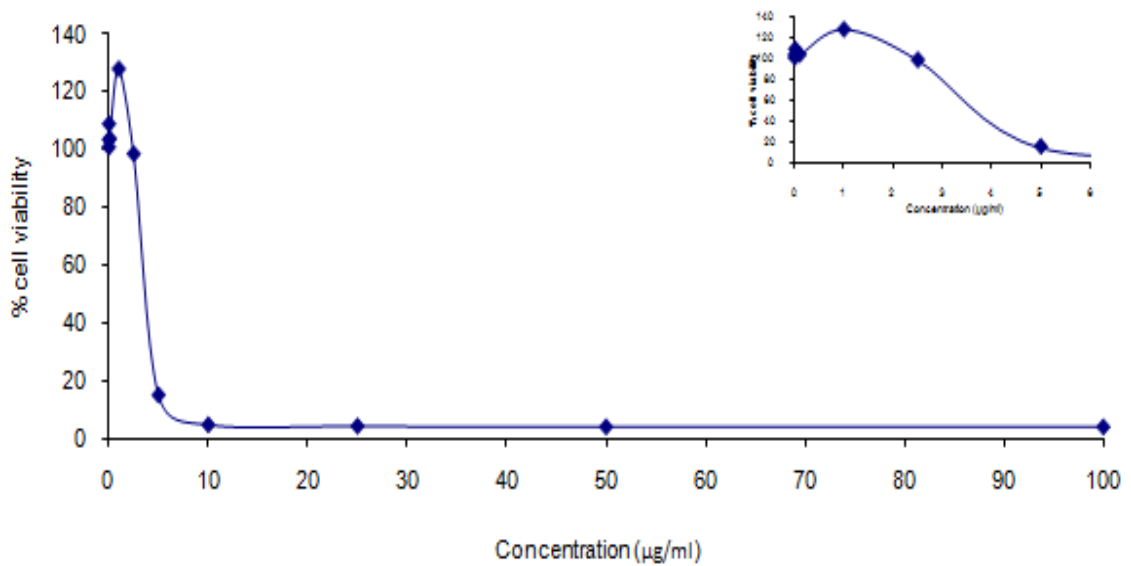


Figure 2.23. MTT results for red CdTe / CdS quantum dots in PC3 cells for 2 days

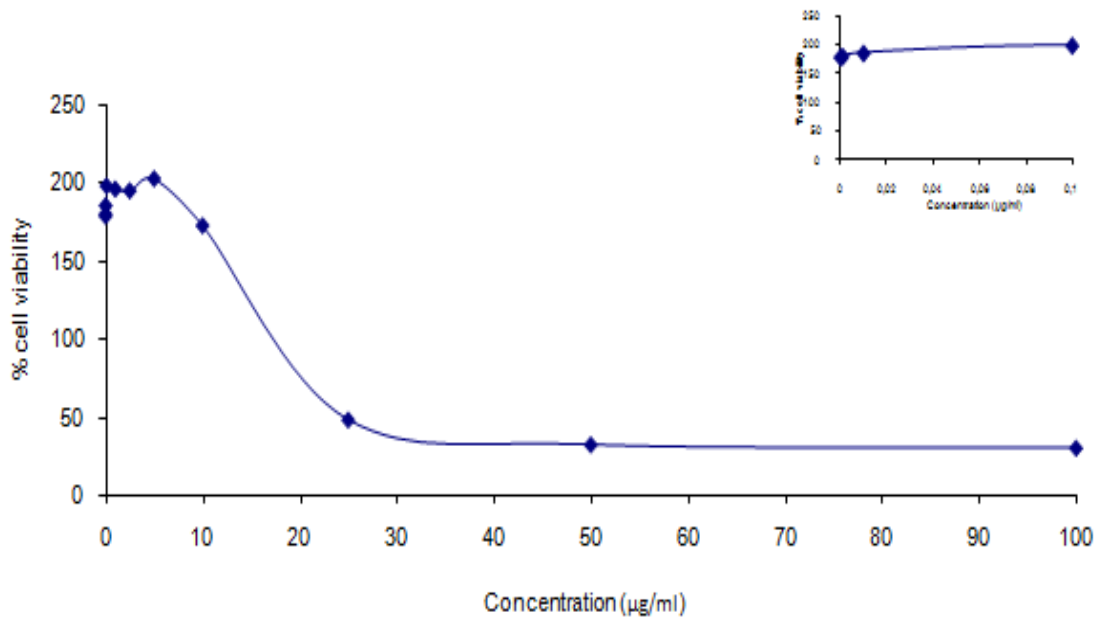


Figure 2.24. MTT results for CdCl₂ in MCF7 cells for 1 day

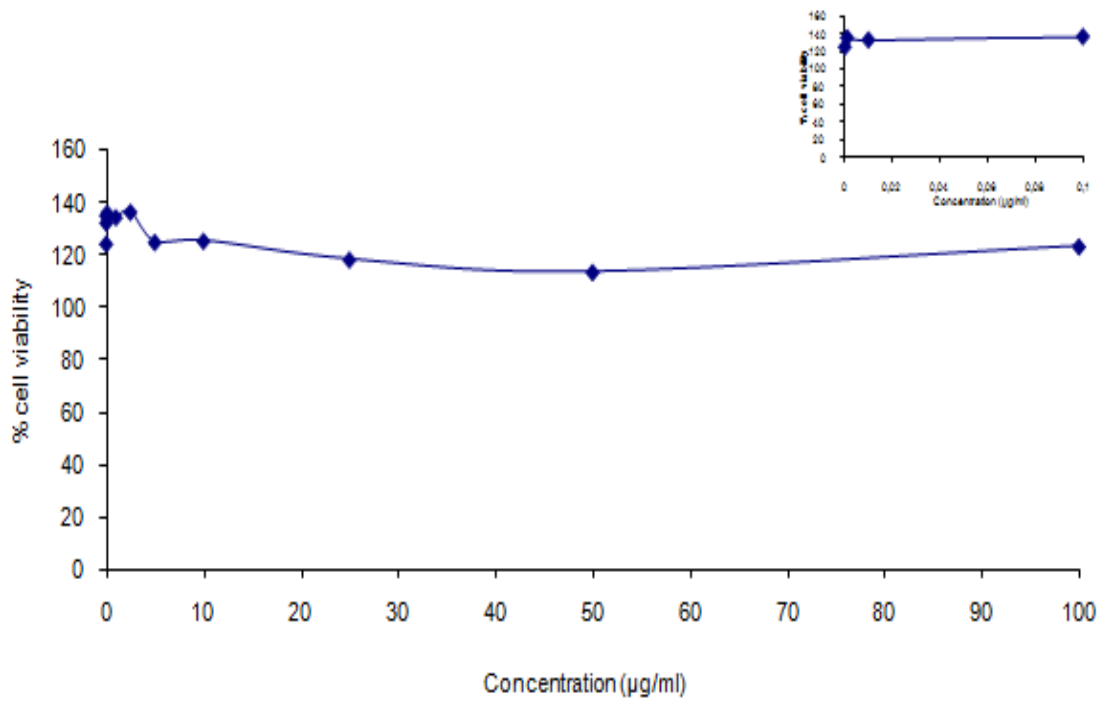


Figure 2.25. MTT results for thiourea in MCF7 cells for 1 day

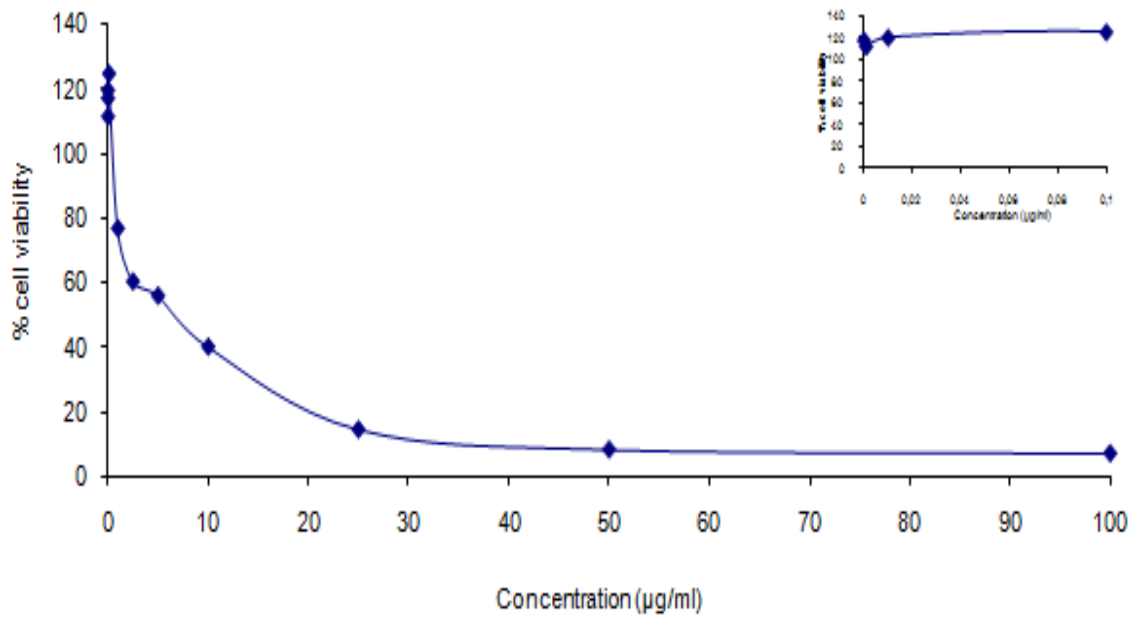


Figure 2.26. MTT results for CdCl₂ in PC3 cells for 1 day

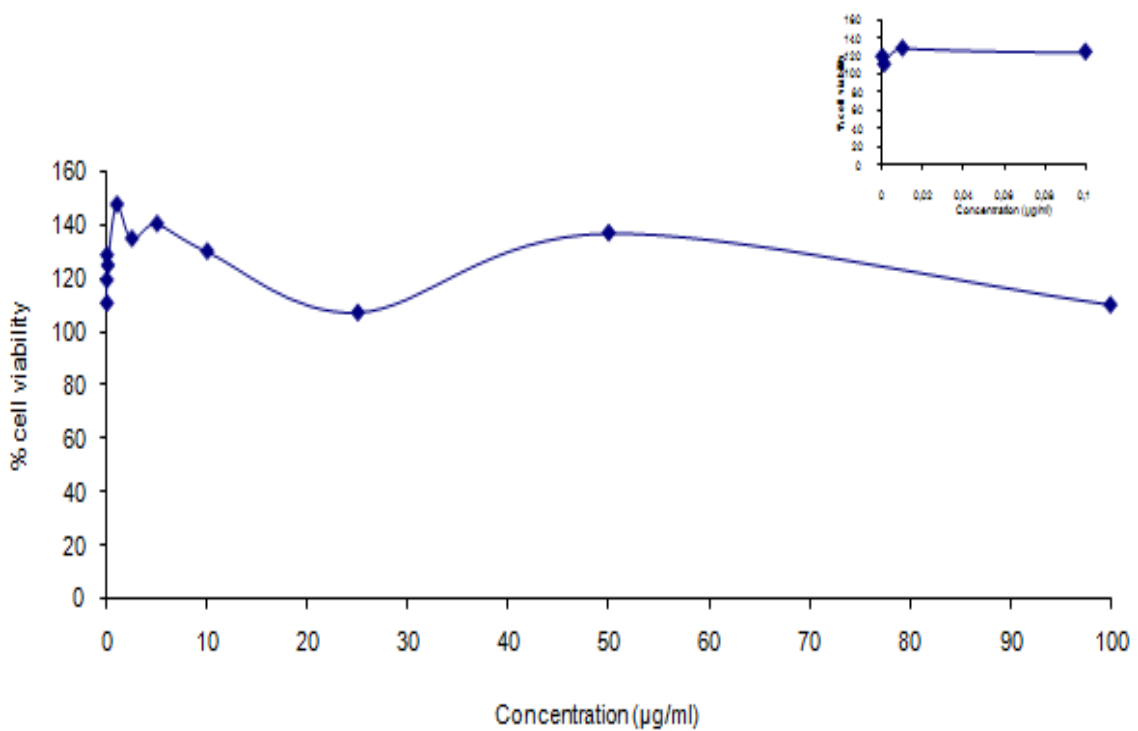


Figure 2.27. MTT results for Thiourea in PC3 cells for 1 day

MTT test results in PC3 and MCF7 cells with red, yellow and green CdTe / CdS nanoparticles, CdCl₂ and thiourea for 1 day and 2 days are represented in this section. As free Cd²⁺ source, CdCl₂ is used and lethal concentration is observed around 15 µg/ml for MCF7 cells and 2.5 µg/ml for PC3 cells (Figure 2.24, Figure 2.26). As S source, thiourea is used and it is observed that thiourea is not toxic for MCF7 and PC3 cells (Figure 2.25, Figure 2.27). For PC3 cells, CdTe / CdS nanoparticles are more toxic than for MCF7 cells (from Figure 2.12 to Figure 2.23) (Table 2.5). Also, green CdTe / CdS nanoparticles are seemed to be more toxic than yellow and red CdTe / CdS nanoparticles (from Figure 2.12 to Figure 2.23). As usual, nanoparticles are more toxic for cells when they are treated with cells for 2 days than when they are treated with cells for 1 day (from Figure 2.12 to Figure 2.23). For fluorescence microscope applications, maximum 1 µg/ml concentration is seemed to be ideal for PC3 cells and maximum 30 µg/ml concentration is seemed to be ideal for MCF7 cells (from Figure 2.12 to Figure 2.23) (Table 2.5). Lethal concentrations are determined by determining the concentration of CdTe / CdS nanoparticle where cell viability is 50 % (from Figure 2.12 to Figure 2.27).

Table 2.5.MTT Test results for CdTe / CdS nanoparticles, CdCl₂ and Thiourea in MCF7 and PC3 Cells

Sample Name	Lethal Concentration for MCF7 (µg/ml)		Lethal Concentration for PC3 (µg/ml)		Ideal concentration range for Fluorescence studies for MCF7 (µg/ml)	Ideal concentration range for Fluorescence studies for PC3 (µg/ml)
	1Day	2 Days	1 Day	2 Days		
Thiourea	Non Toxic	---	Non Toxic	---	---	---
CdCl ₂	15	---	2.5	---	---	---
Green CdTe / CdS nanoparticles	25	15	1,5	1	0.0001- 30	0,0001-1
Yellow CdTe / CdS nanoparticles	Non Toxic	Non Toxic	2.5	2	0.0001- 100	0,0001-3
Red CdTe / CdS nanoparticles	Non Toxic	Non Toxic	3	5	0.0001- 100	0,0001-5

2.2.3.2. Fluorescence Confocal Microscope images

CdTe / CdS nanoparticles with different sizes were incubated for two hours with hepatocytes cells in PBS. Concentration of nanoparticles was 1 $\mu\text{g/ml}$ following MTT results. Cells were fixed with paraformaldehyde and observed under fluorescence confocal microscope with 488 nm laser light. For Green CdTe / CdS nanoparticles 510 nm – 530 nm, for yellow CdTe / CdS 580 nm – 610 nm, for red CdTe / CdS nanoparticles 640 nm – 680 nm ranged emission filters are used in confocal microscopy Figure 2.28., Figure 2.29., Figure 2.30., shows confocal images of liver cancer cells labelled with different sized CdTe / CdS nanoparticles under fluorescence confocal microscope. CdTe / CdS nanoparticles with various size nearly similar images were observed with. For all cases, CdTe / CdS nanoparticles penetrate into cell and disperse in cell cytoplasm, however they do not enter the nucleus of liver cells. The brightness of these images were changed with the CdTe / CdS nanoparticles having different quantum yield. The yellow light emitting CdTe / CdS nanoparticles exhibit the brightest image among them. In addition, more punctuates within the cells are observable, indicating that a lot of nanoparticles are internalized.

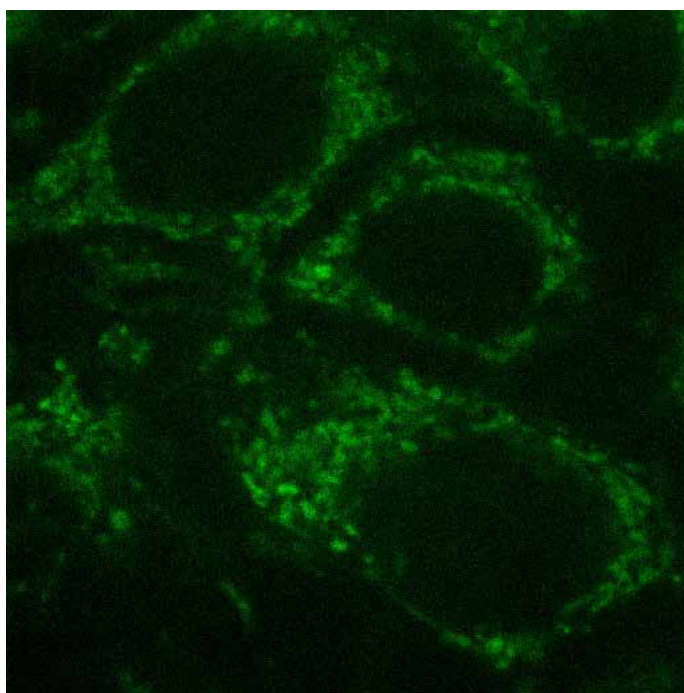


Figure 2.28. Colored fluorescence confocal microscope image of green light emitting CdTe / CdS in liver cancer cells

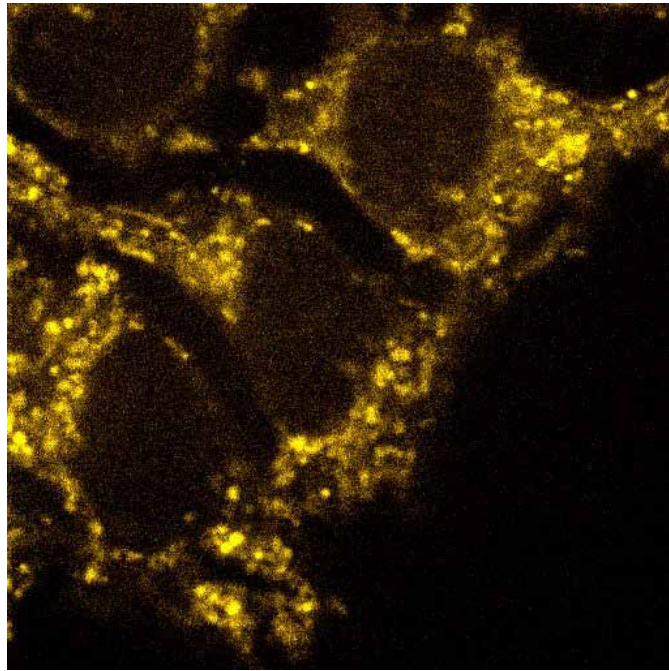


Figure 2.29. Colored fluorescence confocal microscope image of yellow light emitting CdTe / CdS in liver cancer cells

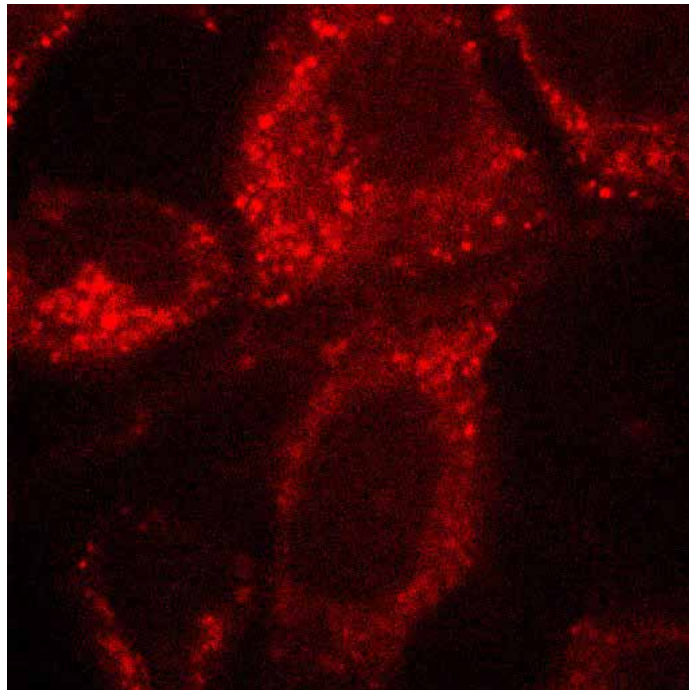


Figure 2.30. Colored fluorescence confocal microscope image of red light emitting CdTe / CdS in liver cancer cells

2.3. Discussion

Color change in CdTe / CdS observed in this work was convenient with literature (Wuister, et al. 2003, Zhong, et al. 2008, Gaponik, et al. 2002, Peng, et al. 2007). Zhong et.al mentioned that color of the CdTe / CdS nanoparticles changes by time from green to red to green because the conduction and valance band in quantum dots get closer when quantum dots get bigger and emission spectra of quantum dots are red shifted (Zhong, et al. 2008). In this study, green, yellow and red colors were clearly observed due to change in size of CdTe / CdS nanoparticles.

The growth rate of CdTe / CdS nanoparticles was agreed with the literature (Qian, et al. 2007). Zhong et.al mentioned that the growth rate of CdTe / CdS nanoparticles changes with the ratio of Te:S. However, in this study growth rate of CdTe / CdS was much slower than the report of Zhong et al. (Zhong, et al. 2008). The reason might be the amount of Te used during the synthesis. Qian et.al synthesized CdTe nanoparticles with nearly same method as Zhong et.al.'s study (Qian, et.al 2007). However, in this study, the amount of Te used was very small when it is compared to Zhong et.al.'s study (0.008 mmol in our study, 0.02 mmol in Zhong et al.'s study). In this study, amount of Te used was around same amount with Qian et.al.'s study. The growth rates of CdTe / CdS nanoparticles in both studies are parallel to each other, which means, they are similar. Also the growth rate of CdTe / CdS nanoparticles in this study is slowing down when nanoparticles get bigger. The reason for this behavior might be the time which is needed to cover bigger quantum dots is longer than the time which is needed to cover smaller quantum dots.

At shorter wavelengths, FWHM of CdTe / CdS nanoparticles were narrower, around 50 nm; however when the emission peaks are red shifted, FWHM of CdTe / CdS nanoparticles are broadened, around 100 nm. The reason for this increment may be due to polydispersity of CdTe / CdS nanoparticles. In Zhong et.al.'s study, FWHM of CdTe / CdS nanoparticles vary between 35 nm and 55 nm (Zhong, et al. 2008). Gaponik et.al indicated that FWHM of CdTe nanoparticles may increase to 60 nm with the increment in size (Gaponik, et al. 2002). Qian et.al. mentioned 80 nm of FWHM is considered to be normal (Qian, et.al 2007). In this study, FWHM of green CdTe / CdS (50 nm) is compareable, however, the red CdTe nanoparticles, FWHM value shows a large

deviation from the value of 60 nm to 100 nm. We conclude that in our study, monodispersity of CdTe / CdS nanoparticles is reduced within increased reaction time. Because of continue of nucleation of nanocrystals during reaction, the monodispersity of CdTe / CdS nanoparticles is reduced when particles get bigger. When nanocrystals get bigger, also new smaller nanocrystals occur, and this leads to more polydispersity in bigger nanocrystals.

Qian et.al. mentioned that Stokes shift of CdTe nanoparticle decreases as nanoparticles get bigger (Qian, et.al 2007). Rogach et.al. did not corrolate Stokes shift with size, however, claimed that Stokes shift can correlate with quantum yields (Rogach, et al. 2007). In this study, Stokes shifts of CdTe / CdS nanoparticles increase as the size of nanoparticles increases. The results show that, surface coating of nanoparticles in bigger nanoparticles is not as good as that in smaller nanoparticles. This situation can be corrected by adding appropriate amount of surfactant into reaction media; however this addition may cause problems in purification step.

The quantum yields of CdTe / CdS nanoparticles are highly sensitive to change in particle's size. Zhong et.al. indicated that quantum yield of CdTe / CdS nanoparticles increases with size of nanoparticles, however, it starts decreasing when the particles emitting red light. When the size of nanoparticle become closer to bulk, quantum yield decreases (Zhong, et al. 2008). In our study, fluorecence quantum yield arise until CdTe / CdS nanoparticles emit yellow color, however, was decreased rapidly with red color. Quantum yield of nanoparticles were around 30 % at yellow color. Zhong et.al. mentioned that quantum yield of CdTe / CdS nanoparticles may arise to 80 % (Zhong, et al. 2008). In comparison, the nanocrystals synthesized in this study are less brighter. Quantum yield of nanoparticles is strongly depends on coordination in crystal structure. In smaller nanoparticles, the crystal structure is not formed perfectly, so quantum yield is not high. Within increased reaction time, quantum dots get bigger and when quantum dots get bigger, the crystal structure takes shape better and defects are gone, so quantum yield gets higher. However, when quantum dots get much bigger, this time the surface of nanoparticles start to deform and structural defects occur, nanoparticles tend to agglomerate, and quantum yield of nanoparticles decrease.

Our XRD studies agree with the literature. Zhong et.al and Gaponik et.al mentioned that CdTe nanoparticles have cubic structure (Zhong, et al. 2008, Gaponik, et al. 2002). Different from bulk crystals; XRD peaks in nanocrystals are broader. Due to Debye – Scherrer rule, broadening in XRD peaks of crystals is caused by decrease in

size of crystals. In this study, crystal structure of CdTe / CdS nanoparticles is determined to be face centered cubic. Size of CdTe / CdS nanoparticles is varied between 5 nm – 10 nm. These values are in the range reported in the literature (Zhong, et al. 2008, Gaponik, et al. 2002). Also, size is estimated from the band gap energies of nanoparticles determined from UV – Vis spectroscopy. However, these theoretical sizes determined from the equation 2.2 are bigger than the sizes that are determined from XRD studies. However, UV – Vis spectroscopy is not generally used for size determination for CdTe nanoparticles, the sizes determined from XRD are more trustable values when they are compared with literature (Zhong, et al. 2008, Gaponik, et al. 2002, Qian, et al. 2007)

Core – shell structure of CdTe / CdS nanoparticles can be proved by XRD studies. In this study, XRD peaks of CdTe / CdS nanoparticles shifted to larger angles when the particles get bigger. If it were a core CdTe nanoparticle, the XRD peaks should not shift to the longer wavelengths, they should remain constant. The shift of nanoparticles to the bigger angles shows that CdS grows epitaxial around CdTe core. XRD peaks of nanoparticles located between CdTe and CdS phase, which agrees with the smaller lattice constant for CdS compared with CdTe. (Zhong, et al. 2008)

Hydrodynamic radius of nanocrystals is bigger than the size estimated by UV – Vis spectroscopy and XRD. Nanocrystals are surrounded by surfactants, such as 3 – MPA or thioglycolic acid, causes increase in size of nanocrystals. In this study, the crystal size of nanocrystals were determined from XRD are between 5 nm and 10 nm. However, the size of nanocrystals with surfactant, which is 3 – MPA, is around 15 nm.

ICP – MS analyses showed CdTe / CdS nanoparticle size is independent from the amount of Te. Moreover, an increase in Cd concentration due to increase in nanoparticle size shows that CdTe core is surrounded by CdS shell.

Fluorescence confocal microscopy shows that the nanoparticles can interact with cancer cells of liver. These results show 3 – MPA capped CdTe / CdS nanoparticles enter cell and stays in cytoplasm. These results indicate that 3 –MPA capped CdTe / CdS nanoparticles can be used in cell bioimaging applications. 3 – MPA binds nanocrystal from S and COOH side of 3 – MPA remains free, so nanoparticles in cell cytoplasm can attach any protein or amine group. However, CdTe / CdS nanoparticles could not enter nucleus, because the hydrodynamic size of the nanoparticles is bigger than size of nucleus hole (Lovric, et al. 2005).

From MTT test results, it is found that toxicity of nanoparticles differs from in different cells and with different sizes. The most toxic type of CdTe / CdS nanoparticles

are the smallest CdTe / CdS nanoparticles, the green light emitting CdTe / CdS nanoparticles. Yellow and red light emitting CdTe / CdS nanoparticles followed green light emitting CdTe / CdS nanoparticles respectively. The reason for high toxicity of green light emitting CdTe / CdS nanoparticles might be the amount of free Cd²⁺ in green light emitting CdTe / CdS nanoparticles. From ICP - MS analysis, it is observed that green light emitting CdTe / CdS nanoparticles have the least amount of Cd, however, probably green light emitting CdTe / CdS nanoparticles are not stable and tend to dissociate to free Cd and Te immediately. It is observed that green light emitting CdTe / CdS nanoparticles are more toxic than even CdCl₂, which is source of free Cd²⁺. In PC3 cells, CdTe / CdS nanoparticles are more toxic than they are in MCF7 cells. Red and yellow CdTe / CdS nanoparticles are not toxic for MCF7 cells at all, where CdCl₂ is toxic around 15 µg / ml for MCF7 cells. S source thiourea is non – toxic when its concentration is lower than 100 µg / ml. Derfus et al. made a study on cytotoxic effects of core CdSe quantum dots in rat primary hepatocytes and found out that CdSe core quantum dots undergo surface oxidation, resulting in the release of free cadmium ions. Cadmium ions cause damage in mitochondria and oxidative stress in cells, for that reason it is considered to be toxic (Derkus, et al. 2004). However, this surface oxidation was prevented with coating core surface with different material, by this way cadmium was imprisoned in core structure and remained bound to selenium. This was demonstrated with the addition of a ZnS shell; the oxidative degradation of the CdSe core due to exposure to air was significantly reduced resulting in lower cytotoxicity (Derkus, et al. 2004).

2.4. Conclusion

Highly luminescent and water soluble CdTe / CdS nanoparticles are synthesized by one pot aqueous synthesis method. Crystal structure of these nanoparticles is estimated to be face centered cubic and the size of these nanoparticles varies between 5 nm and 10 nm where hydrodynamic radius is around 15 nm. 3 – MPA capped CdTe / CdS nanoparticles enter and stay in cell cytoplasm without killing cells. These nanoparticles were successfully displayed by fluorescence confocal microscope and it is shown that 3 – MPA capped CdTe / CdS nanoparticles are suitable for cell imaging applications. MTT tests proved that toxicity of CdTe / CdS nanoparticles changes with

nanoparticle size and cell type. However, for all cases, below 1 μ g/ml nanoparticle concentration CdTe / CdS nanoparticles are not toxic and 1 μ g/ml concentration is suitable for fluorescence microscopy studies.

CHAPTER 3

DEVELOPMENT OF CdSe_xS_{1-x} QUANTUM DOTS

3.1. Experimental

CdSe nanoparticles are widely synthesized by organometallic synthesis method. Recently Pan et.al. described an alternative two – phase method for synthesizing CdSe and CdSe / CdS nanoparticles. With a slight modification in CdSe / CdS nanoparticle synthesis by two phase method, CdSe_xS_{1-x} nanoparticles are synthesized. In this chapter, synthesis and characterization of CdSe_xS_{1-x} nanoparticles are discussed.

3.1.1. Synthesis of Cadmium Myristate

10 mmoles of Cadmium oxide (CdO) and 20 mmoles myristic acid (Figure 3.1) were put into a 50 ml reaction flask and heated at 200 °C for ten minutes. As a result, a clear solution was obtained. Cadmium myristate (Figure 3.2) was recrystallized in toluene and used for further experiments.

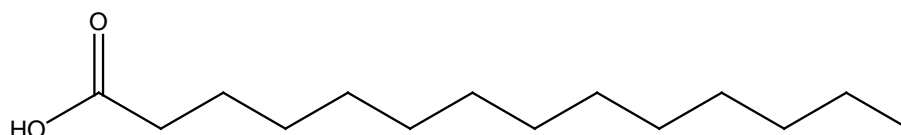
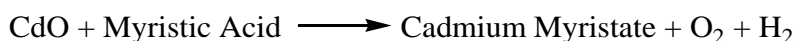


Figure 3.1. Structure of myristic acid

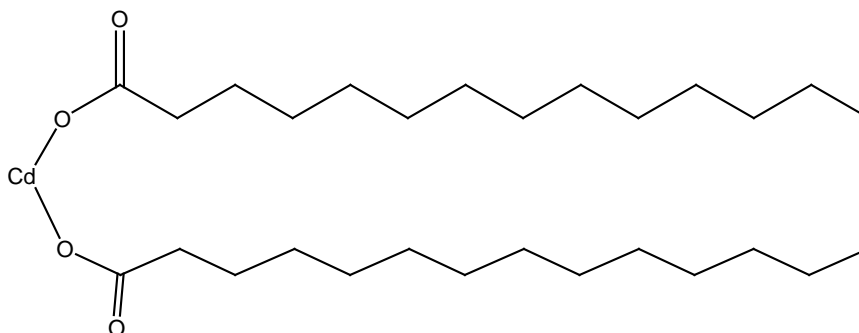


Figure 3.2. Structure of Cadmium Myristate

3.1.2. Synthesis of NaHSe as Se precursor

Se powder (0.4 mmol) and NaBH₄ (1 mmol) were put into 5 ml reaction flask under N₂ atmosphere. Then 1 ml of distilled water added to the reaction flask. The solution in N₂ atmosphere is allowed to react to form a white precipitate, Na₂B₄O₇. Then resulting clear solution transferred into another degassed test tube. No other purification techniques were performed. In all experiments, freshly synthesized NaHSe was used and synthesized NaHSe was not stored for other experiments (Klayman et.al, 1972). The reaction is considered to be as below;



3.1.3. Synthesis of CdSe_xS_{1-x} nanoparticles

CdSe_xS_{1-x} nanoparticles were synthesized according to a modified technique based on two – phase synthesis method.(Pan, et al. 2005) First, cadmium myristate (CdMA) (0.4 g) was dissolved in toluene (80 ml) with oleic acid (OA) (2 g) or TOPO (2 g) at 80 °C, and stored for next the step. NaHSe (3 mg) and Thiourea (60 mg) were dissolved in water (80 ml) and heated to 100 °C under N₂ atmosphere for 30 minutes. Temperature was kept constant at 100 °C and the solution was stirred vigorously. While stirring, the toluene solution was added to the water solution and reaction started. After 30 minutes, CdSe_xS_{1-x} quantum dots started to grow (Figure 3.3). Aliquots of sample were taken at different time intervals and their optical properties were analyzed by using UV – vis and fluorescence spectroscopies. Reaction was stopped at desired time by cooling the final solution. Nanoparticles were precipitated by addition of the ethanol in to the crude solution of nanoparticles. Precipitation procedure was repeated several times to remove impurities and excess capping agent.

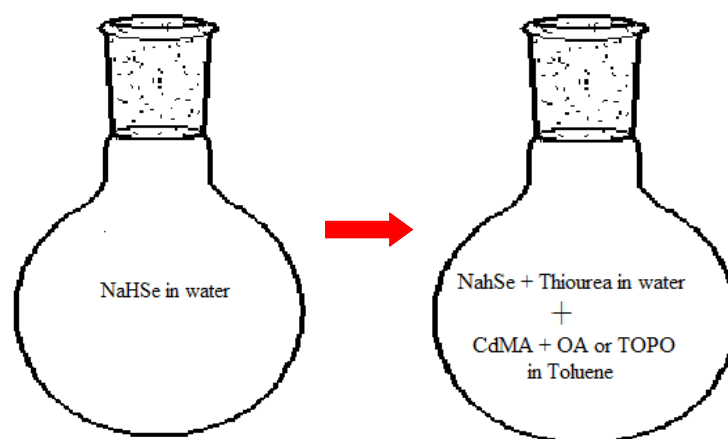


Figure 3.3. Schematic Illustration of Synthesis of $\text{CdSe}_x\text{S}_{1-x}$

3.1.4. Ligand Exchange for $\text{CdSe}_x\text{S}_{1-x}$ quantum dots

To exchange a ligand, a method from literature was modified (Zhang, et al. 2008). Solid $\text{CdSe}_x\text{S}_{1-x}$ nanoparticles were dispersed in chloroform and 3 – MPA was dissolved in distilled water, and pH of water solution was adjusted to 10 by adding 1 M NaOH. Then two solutions were mixed together and shaken for 2 days at room temperature. After 2 days, water and chloroform phases were separated. Optical characterization for aqueous solution was performed by using fluorescence spectrum.

3.2. Characterization

3.2.1. Optical characterization

Optical characterization of $\text{CdSe}_x\text{S}_{1-x}$ nanocrystals were carried out by using UV – Vis absorption and fluorescence spectroscopies. In Figure 3.4, the temporal growth of $\text{CdSe}_x\text{S}_{1-x}$ nanocrystals with a mole ratio of Se : S of 1 : 20.

Due to extended reaction time, the fluorescence spectra shift to higher wavelengths, indicating the growth of nanoparticles.(Figure 3.4)

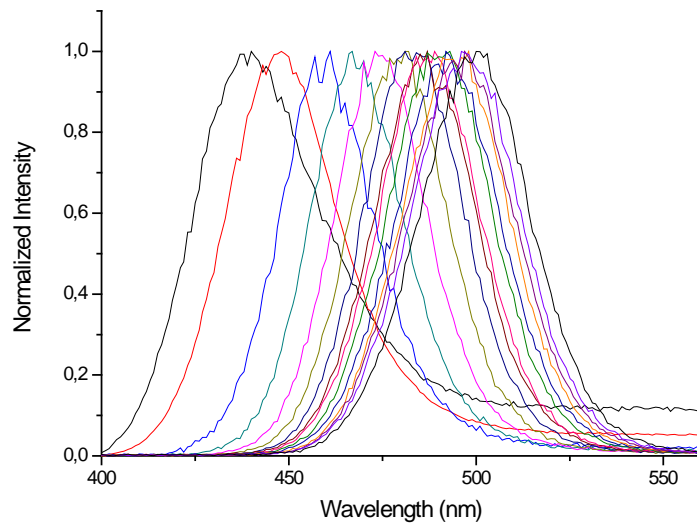


Figure 3.4. Fluorescence spectrum of $\text{CdSe}_x\text{S}_{1-x}$ nanoparticles synthesized at different time intervals (from 0.5 hour to 13 hours)

In Figure 3.5, the growth of $\text{CdSe}_x\text{S}_{1-x}$ nanoparticles are shown. The growth of $\text{CdSe}_x\text{S}_{1-x}$ depends on time. As seen from the Figure 3.5, the rate is faster upto 300 minutes (5 hours) and then it slows down and saturates around 10 hours.

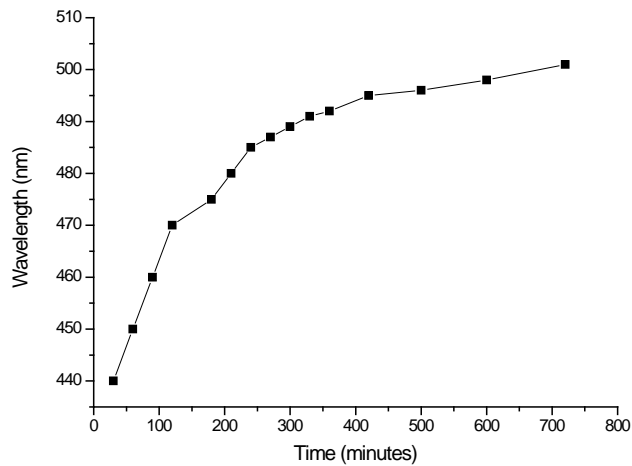


Figure 3.5. Temporal evolution of fluorescence peaks of $\text{CdSe}_x\text{S}_{1-x}$ nanoparticles

Also it is possible to grow $\text{CdSe}_x\text{S}_{1-x}$ nanoparticles with different molar ratios of Se:S. Figure 3.6 and Figure 3.7 show the growth of $\text{CdSe}_x\text{S}_{1-x}$ nanoparticles with Se:S mole ratio of 1:30. The growth behavior for this ratio is totally different than the mole

ratio of Se: S of 1:20. It indicates that the mole ratio is an important parameter for the growth.

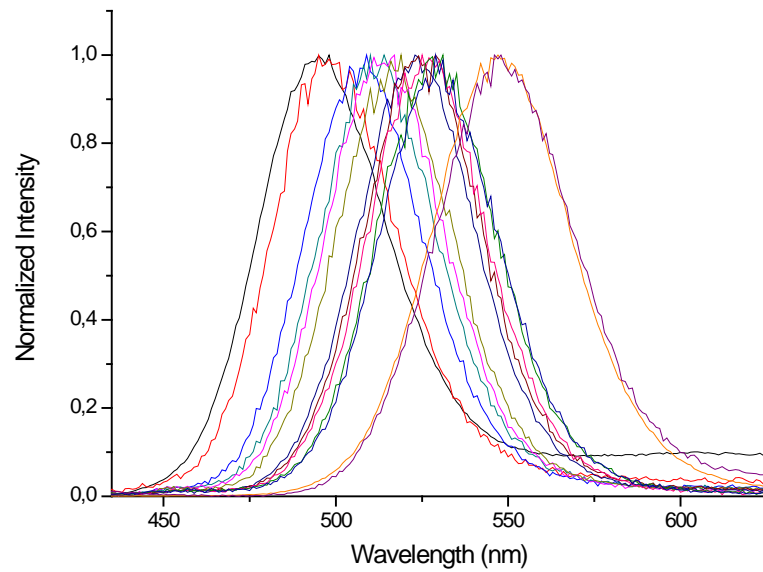


Figure 3.6. Fluorescence spectrum of CdSe_xS_{1-x} nanoparticles synthesized at different time intervals (from 0.5 hour to 15 hours)

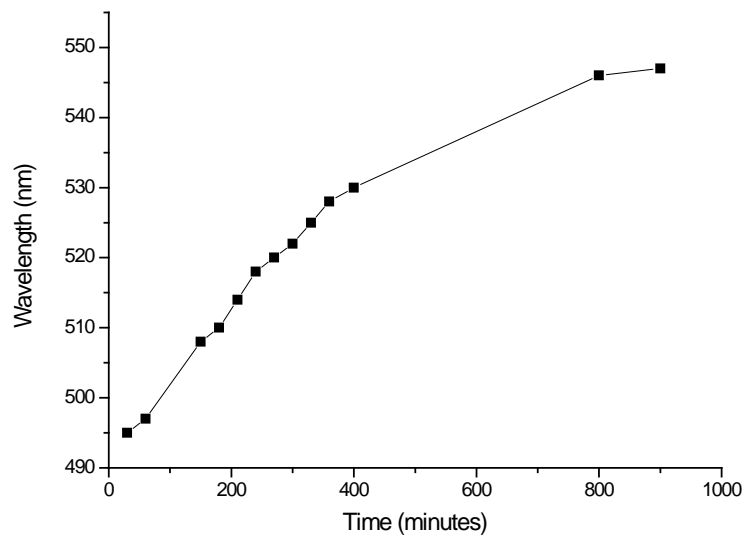


Figure 3.7. Temporal evolution of fluorescence peaks of CdSe_xS_{1-x} nanoparticles

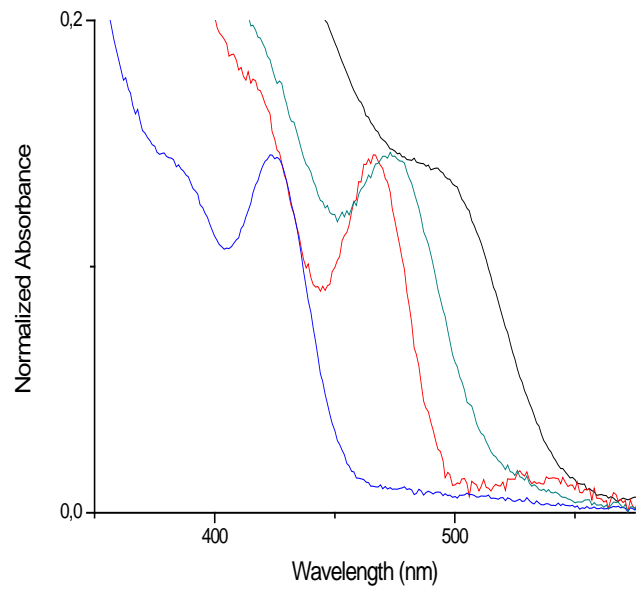


Figure 3.8. UV – vis spectra of CdSe_xS_{1-x} quantum dots

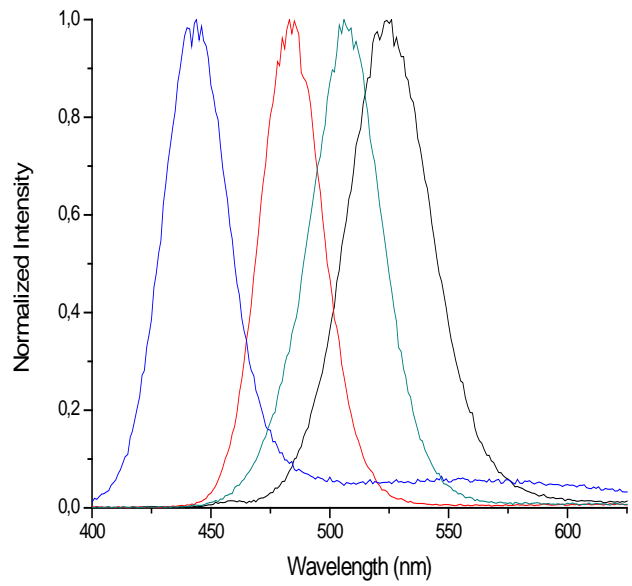


Figure 3.9. Fluorescence spectra of CdSe_xS_{1-x} quantum dots



Figure 3.10. Luminescence image of $\text{CdSe}_x\text{S}_{1-x}$ nanoparticles under UV lamp

Figure 3.8 and Figure 3.9 shows temporal evolution of $\text{CdSe}_x\text{S}_{1-x}$ nanocrystal by using UV – Vis and fluorescence spectrometers. Figure 3.10 shows luminescence image of different $\text{CdSe}_x\text{S}_{1-x}$ under UV irradiation.

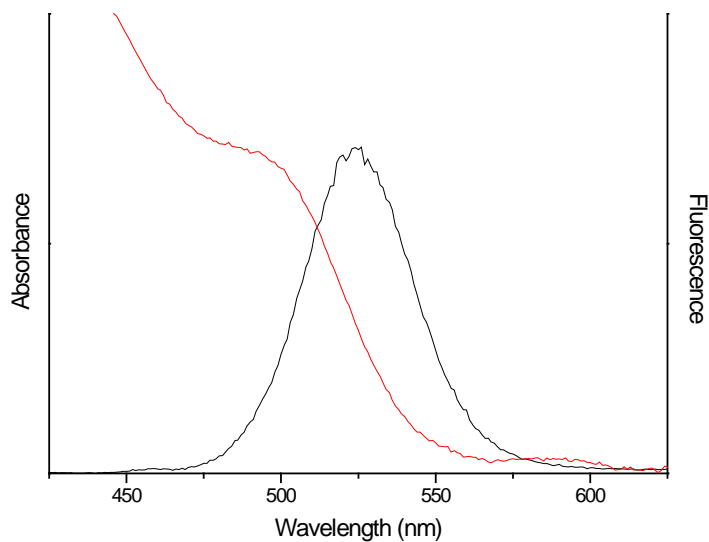


Figure 3.11. Fluorescence and UV – vis spectra of $\text{CdSe}_x\text{S}_{1-x}$ nanoparticles (Emission 525 nm)

Stokes shift and FWHM of $\text{CdSe}_x\text{S}_{1-x}$ nanoparticles are calculated and tabulated (Table 3.1). The FWHM become broader when particles get bigger also the stokes shift increases with increase in particle size.

Quantum yield (QY) of this nanoparticles are calculated by using Rhodamine 6G in water (QY: %95) as reference at 400 nm excitation wavelength. Table 3.1 shows photophysical properties of CdSe_xS_{1-x} nanocrystals

Table 3.1. Photophysical properties of CdSe_xS_{1-x} nanocrystals

Sample Name	$\lambda_{\text{absorption}}$ (nm)	$\lambda_{\text{fluorescence}}$ (nm)	Stokes Shift (nm)	FWHM (nm)	QY (%)	E_g	
						(nm)	(eV)
CdSe _x S _{1-x} 1	423	445	22	29	45	455	2.7
CdSe _x S _{1-x} 2	466	485	19	30	75	496	2.5
CdSe _x S _{1-x} 3	476	505	29	36	80	515	2.4
CdSe _x S _{1-x} 4	495	525	30	40	80	540	2.3

CdSe_xS_{1-x} nanocrystals are dispersible in oil (toluene, heptane, etc...). By ligand exchange these quantum dots can be dispersible in water, however, optical properties of this nanocrystals differ after ligand exchange treatment. Figure 3.12 and Figure 3.13 shows optical changes in CdSe_xS_{1-x} nanocrystals after ligand exchange. Optical changes are tabulated in Table 3.2. The properties are dramatically changed. The QY of water soluble nanoparticles is decreased by 10 – fold; the FWHM is broadened 5 times; these results indicate that the ligand exchange yields an important change in structure of the nanoparticles.

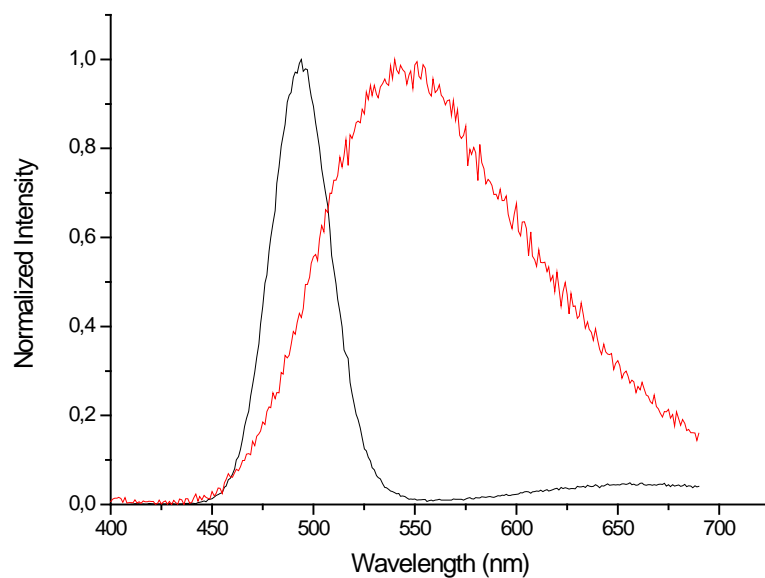


Figure 3.12. Fluorescence wavelength change after ligand exchange

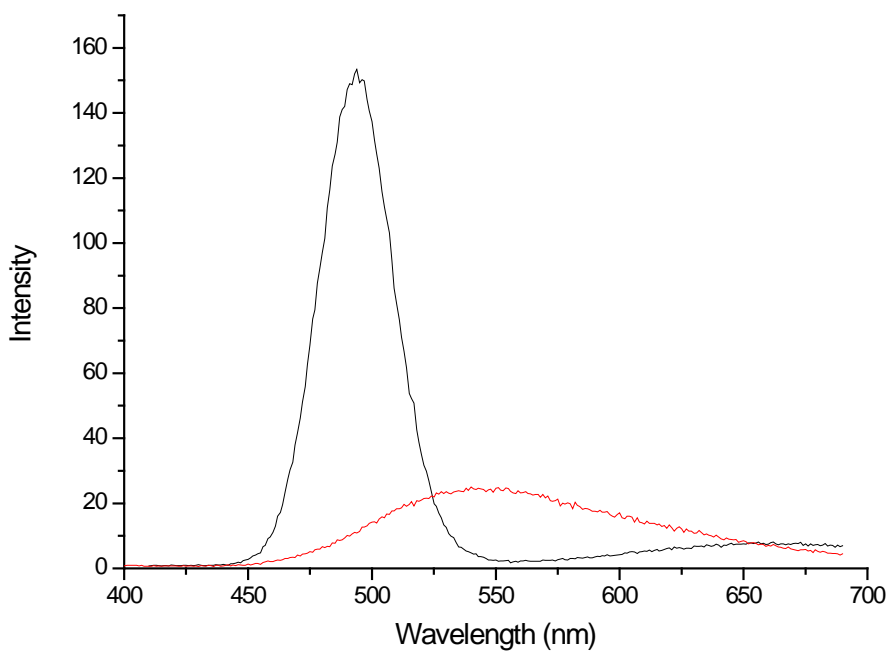


Figure 3.13. Fluorescence intensity change after ligand exchange

Table 3.2. Optical Changes after ligand exchange

Sample Name	$\lambda_{\text{fluorescence}}$	FWHM	QY
TOPO capped CdSe _x S _{1-x}	495 nm	20 nm	75%
MPA capped CdSe _x S _{1-x}	545 nm	100 nm	7%

3.2.2. Structural Characterization:

TEM and XRD analysis are made for CdSe_xS_{1-x} nanocrystals. Figure 3.14 and Figure 3.15 show TEM images of CdSe_xS_{1-x} nanoparticles. From TEM analysis, particle size is determined to be 4.7 nm. The particles are monodisperse with face centered cubic crystal structure.

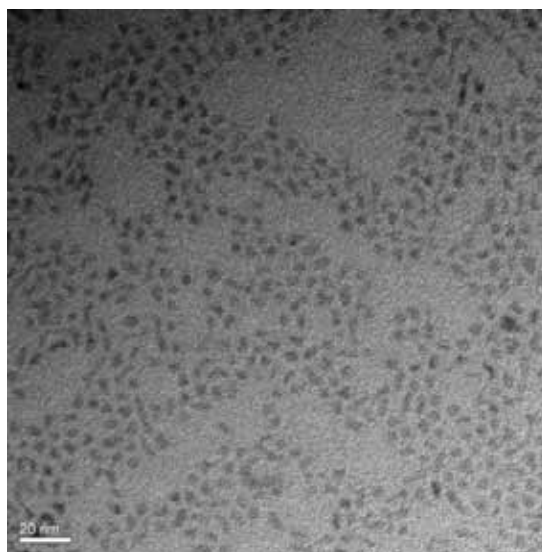


Figure 3.14. TEM images of CdSe_xS_{1-x} nanoparticles (20 nm scale)

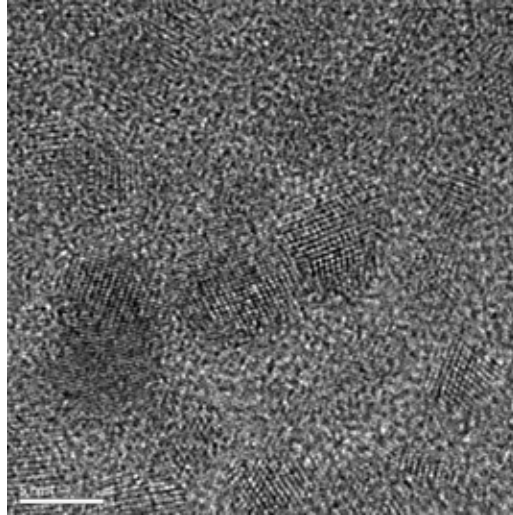


Figure 3.15. TEM images of $\text{CdSe}_x\text{S}_{1-x}$ nanoparticles (5 nm scale)

Figure 3.16 shows XRD analyze of green and purple light emitting $\text{CdSe}_x\text{S}_{1-x}$ nanoparticles. By comparing bulk CdS and CdSe bulk structures hkl indices, $\text{CdSe}_x\text{S}_{1-x}$ nanoparticles crystal structure is estimated to be face centered cubic. Particle size of $\text{CdSe}_x\text{S}_{1-x}$ nanoparticles are calculated from Debye – Scherrer equation (Equation 1.11). Size of $\text{CdSe}_x\text{S}_{1-x}$ nanoparticles are estimated to be around 3.5 nm.(Table 3.3)

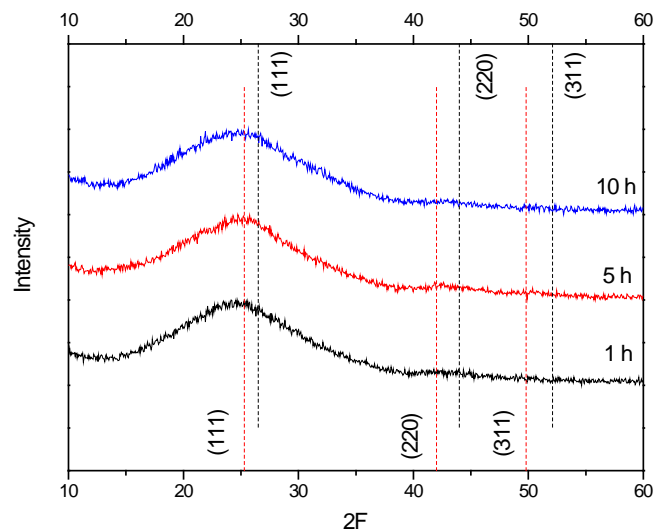


Figure 3.16.XRD spectra of purple, blue and green emitting $\text{CdSe}_x\text{S}_{1-x}$ nanoparticles, red dots hkl indices of cubic bulk CdSe (bottom), black dots hkl indices of cubic bulk CdS (top)

Size of nanoparticles can also be determined from UV – Vis spectroscopy by using Equation 1.8. From literature, E_{gb} of CdSe is found to be 1.73 eV, m_e of CdSe is $0.11 m_0$, m_h of CdSe is $0.45 m_0$ and ϵ is $9.6 \epsilon_0$ (m_0 is free electron mass and ϵ_0 is vacuum dielectric constant) (Joshi, et al. 2006, Banerjee 2000). By putting these values into equation 1.8, the second order equation below is determined,

$$\frac{1878}{\lambda} = 2.79 + 48.7 \frac{1}{d^2} - 0.868 \frac{1}{d} \quad (3.1)$$

where λ is first exciton peak cutting through wavelength axis in absorption spectrum and d is diameter of nanoparticle. By solving this 2nd order equation, the equation below is determined,

$$\frac{1}{d} = 0.0089 + \sqrt{\frac{38.56}{\lambda} - 0.057} \quad (3.2)$$

The sizes determined from absorbance spectroscopy is different from the ones that are determined by using TEM and XRD. From UV – vis spectrum analysis, the size of nanoparticles are found to be bigger.(Table 3.3)

Table 3.3.Size determination of CdSe_xS_{1-x} nanoparticles from TEM, XRD and UV – Vis Spectroscopy

Sample Name	Nanoparticle size determined by TEM (nm)	Nanoparticle size determined by XRD (nm)	Nanoparticle size determined by UV – vis spectroscopy (nm)
CdSe _x S _{1-x} 1	---	3.5	5.7
CdSe _x S _{1-x} 2	---	3.6	6.5
CdSe _x S _{1-x} 3	---	3.7	7.0
CdSe _x S _{1-x} 4	4.7	---	7.4

Also, ICP – MS analysis of $\text{CdSe}_x\text{S}_{1-x}$ nanoparticles in 1 ppm concentration after ligand exchange is done. For 1 ppm $\text{CdSe}_x\text{S}_{1-x}$ nanoparticles, concentration of Cd and Se is found to be 370 ppb and 11 ppb respectively. Amount of Se is very small when it is compared to amount of Cd.

3.3. Discussion

$\text{CdSe}_x\text{S}_{1-x}$ nanoparticles spectra change with molar ratio of Se to S of nanoparticles. Jang et al. claimed that when the molar ratio of Se to S varies, the size does not change but different colored $\text{CdSe}_x\text{S}_{1-x}$ nanoparticles can be obtained (Jang, et al. 2003). In this study, emission peaks of $\text{CdSe}_x\text{S}_{1-x}$ nanoparticles varied with different Se:S ratio. This result showed that instead of CdSe / CdS nanoparticles, $\text{CdSe}_x\text{S}_{1-x}$ nanoparticles are prepared with this synthesizes method. In the study of Pan et.al first CdSe core is synthesized than it is surrounded with CdS (Pan, et al. 2005) . In our work Se and S precursors were added to reaction media at the same time.

The growth rate of $\text{CdSe}_x\text{S}_{1-x}$ nanoparticles in this study was extremely slow. In two phase synthesis method, slow growth rates are observed (Pan, et al. 2003, Pan, et al. 2006, Pan, et al. 2007). However, in this study the growth rate of $\text{CdSe}_x\text{S}_{1-x}$ nanoparticles was slower than Pan et.al.'s work. This is probably caused by an excess amount of surfactants and smaller amount of NaHSe used in this synthesis. The core of $\text{CdSe}_x\text{S}_{1-x}$ nanoparticles is considered to be CdSe rich because of high reactivity of the NaHSe. Following the formation of core of $\text{CdSe}_x\text{S}_{1-x}$ nanoparticles occur, slowly CdS rich shell grows on core, because of slow decomposition of thiourea.

FWHM of $\text{CdSe}_x\text{S}_{1-x}$ nanoparticles is varied between 19 nm and 30 nm. Pan et.al. mentioned that CdSe / CdS nanoparticles have 30 nm of FWHM (Pan, et al. 2007). Bawendi et.al indicated that FWHM of CdSe / ZnS nanoparticles are smaller than 40 nm (Dabbousi, et al. 1997). These results showed that $\text{CdSe}_x\text{S}_{1-x}$ nanoparticles are highly monodisperse in our work. Pan et.al mentioned that Stokes shift of CdSe / CdS nanoparticles is 15 nm (Zhong, et al. 2008). In this study, Stokes shift of $\text{CdSe}_x\text{S}_{1-x}$ nanoparticles is found to be varied between 20 nm and 30 nm, which are convenient with the literature (Bawendi, et al. 1993, Pan, et al. 2007). However, small difference in Stokes shift indicates that trap states in $\text{CdSe}_x\text{S}_{1-x}$ nanoparticles is more than CdSe /

CdS nanoparticles, use of excess amount of surfactant may be the reason of these trap states.

Quantum yield of $\text{CdSe}_x\text{S}_{1-x}$ nanoparticles is calculated around %80 and agrees with the literature. Qian et.al mentioned that quantum yield of $\text{CdSe}_x\text{S}_{1-x}$ nanoparticles is around 80% (Qian, et al. 2007) and Pan et. al indicated that quantum yield of CdSe / CdS is around 80% (Pan, et al. 2007). Slow growth rate of $\text{CdSe}_x\text{S}_{1-x}$ nanoparticles leads to less flawed crystal structure and less flawed crystal structure results in high quantum yield.

According to TEM and XRD results crystal structure of $\text{CdSe}_x\text{S}_{1-x}$ nanoparticles is face centered cubic and the size of nanoparticles varies between 3 nm and 5 nm. TEM and XRD results are convenient with the literature. Pan et.al indicated that face centered cubic and extremely small CdSe / CdS nanoparticles occur in two phase synthesis method (Pan, et al. 2007, Pan et al. 2006, Qian, et al. 2007).

In XRD spectra of $\text{CdSe}_x\text{S}_{1-x}$ nanoparticles, the diffraction angles do not shift with change with the size of $\text{CdSe}_x\text{S}_{1-x}$ nanoparticles, also FWHM of XRD peaks of $\text{CdSe}_x\text{S}_{1-x}$ nanoparticles do not change with the size of $\text{CdSe}_x\text{S}_{1-x}$ nanoparticles. These results indicates that, the size of nanoparticle do not vary with the size, also the structure is probably $\text{CdSe}_x\text{S}_{1-x}$ instead of CdSe / CdS, if the structure was CdSe / CdS, XRD peaks should move to larger angles with adding extra shell layers on core (Pan, et al.2007, Pan, et al. 2005, Jang, et al. 2003, Zhong, et al. 2008).

Also, the size can be calculated from band gap energies of $\text{CdSe}_x\text{S}_{1-x}$ nanoparticles which are determined from UV – Vis spectroscopy. However, the sizes obtained from UV – Vis spectroscopy are bigger than the sizes obtained from TEM and XRD. By UV – Vis spectroscopy, nanoparticles are assumed to have CdSe cores, which may cause errors in size calculations since the nanoparticles that are synthesized in this study is $\text{CdSe}_x\text{S}_{1-x}$ nanoparticles.

ICP – MS analysis showed that $\text{CdSe}_x\text{S}_{1-x}$ nanoparticles contain trace amount of selenium. This is not a surprising result since Se also added to reaction media in very small amounts during synthesis.

3.4. Conclusion:

Highly luminescent and monodisperse $\text{CdSe}_x\text{S}_{1-x}$ nanoparticles with extremely slow growth rate have been synthesized in this study. Crystal structure of $\text{CdSe}_x\text{S}_{1-x}$ nanoparticles estimated to be face centered cubic and the size of $\text{CdSe}_x\text{S}_{1-x}$ nanoparticles varied between 3 nm and 4.7 nm. Quantum yield of $\text{CdSe}_x\text{S}_{1-x}$ nanoparticles are calculated around %80. These nanoparticles may find applications in lasers, LEDs and solar cells.

REFERENCES

- A.El Moussaouy, D. Bria, A. Nougouai. 2006. Thermal effect on bound exciton in CdTe/Cd_{1-x}Zn_xTe cylindrical quantum dots. *Solar Energy Materials & Solar Cells* 90 : 1403–1412.
- Abhishek Joshi, K. Y. Narsingi, and M. O. Manasreh, E. A. Davis, B. D. Weaver. 2006. Temperature dependence of the band gap of colloidal CdSe/ZnS core/shell nanocrystals embedded into an ultraviolet curable resin. *Applied Physics Letters* 89 : 131907.
- Amy Szuchmacher Blum, Martin H. Moore, and Banahalli R. Ratna. 2008. Quantum Dot Fluorescence as a Function of Alkyl Chain Length in Aqueous Environments. *Langmuir* 24: 9194-9197.
- Andrey L. Rogach, Thomas Franzl, Thomas A. Klar, Jochen Feldmann, Nikolai Gaponik, Vladimir Lesnyak, Alexey Shavel, Alexander Eychmüller, Yuri P. Rakovich, and John F. Donegan. 2007. Aqueous Synthesis of Thiol-Capped CdTe Nanocrystals: State-of-the-Art. *Journal Physical Chemistry C* 111: 14628-14637.
- Austin M. Derfus, Warren C. W. Chan, and Sangeeta N. Bhatia. 2004. Probing the Cytotoxicity of Semiconductor Quantum Dots. *Nano Letters* 4:11-18.
- B. O. Dabbousi, J. Rodriguez-Viejo, F. V. Mikulec, J. R. Heine, H. Mattoussi, R. Ober, K. F. Jensen, M. G. Bawendi. 1997. (CdSe)ZnS Core-Shell Quantum Dots: Synthesis and Characterization of a Size Series of Highly Luminescent Nanocrystallites. *Journal Physical Chemistry B* 101 : 9463-9475.
- Bruchez Jr M, Moronne M, Gin P, Weiss S, Alivisatos AP. 1998. Semiconductor Nanocrystals as Fluorescent Biological Labels. *Science*. 281:2013-2016.
- C. B. Murray and C. R. Kagan and M. G. Bawendi. 2000. Synthesis and characterization of monodisperse nanocrystals and close packed nanocrystal assemblies *Annual Review of Materials Science* 30:545–610.
- C. B. Murray, D. J. Noms, and M. G. Bawendi. 1993, Synthesis and Characterization of Nearly Monodisperse CdE (E = S, Se, Te) Semiconductor Nanocrystallites. *Journal of American Chemical Society* 115: 8706-8715.
- Chan WC, Nie S. 1998. Quantum dot bioconjugates for ultrasensitive nonisotopic detection *Science* 281:2016-2018.
- Ciapetti G, Cenni E, Paratelli L, Pizzoferrato. 1993. Evaluation of cell/ biomaterial interaction by MTT assay *Advanced Biomaterials* 14 : 359 – 364 .

- Cunwang Ge, Min Xu, Jing Liu, Jianping Lei and Huangxian Ju. 2008. Facile synthesis and application of highly luminescent CdTe quantum dots with an electrogenerated precursor. *Chemical Communications*.4 : 450 – 452
- D.V. Talapin, S.K. Poznyak, N.P. Gaponik, A.L. Rogach, A. Eychmueller. 2002. Synthesis of surfacemodified colloidal semiconductor nanocrystals and study of photoinduced charge separation and transport in nanocrystal-polymer composites. *Physica E: Low Dimensional Systems and Nano-structures*. 14:237-241.
- Daniele Gerion, Fabien Pinaud, Shara C. Williams, Wolfgang J. Parak, Daniela Zanchet, Shimon Weiss, and A. Paul Alivisatos. 2001. Synthesis and Properties of Biocompatible Water-Soluble Silica-Coated CdSe/ZnS Semiconductor Quantum Dots, *Journal Physical Chemistry B* 105 : 8861-8871.
- Daocheng Pan, Qiang Wang, Jiebin Pang, Shichun Jiang, Xiangling Ji, and Lijia An. 2006 . Semiconductor “Nano-Onions” with Multifold Alternating CdS/CdSe or CdSe/CdS Structure. *Chemical Materials* 18: 4253-4258.
- Daocheng Pan, Qiang Wang, Shichun Jiang, Xiangling Ji, and Lijia An. 2007. Low-Temperature Synthesis of Oil-Soluble CdSe, CdS, and CdSe/CdS Core-Shell Nanocrystals by Using Various Water-Soluble Anion Precursors. *Journal Physical Chemistry C* 111:5661-5666.
- Daocheng Pan, Shichun Jiang, Lijia An, Bingzheng Jiang. 2004. Controllable Synthesis of Highly Luminescent and Monodisperse CdS Nanocrystals by a Two-Phase Approach under Mild Conditions. *Advanced Materials* 16 :982 – 985
- Daocheng Pan, Qiang Wang, Shichun Jiang, Xiangling Ji and Lijia. 2005. An. Synthesis of extremely small CdSe and Highly Luminescent CdSe/CdS Core-Shell Nanocrystals via a novel Two Phase Thermal Approach. *Advanced Materials* 17:176 – 178.
- Day R.N., Periasamy A., Schaufele F. 2001. Fluorescence resonance energy transfer microscopy of localized protein interactions in the living cell nucleus. *Methods* 25:4–18.
- Derfus A.M., Chan W.C.W., Bhatia S.N. 2004. Intracellular delivery of quantum dots for live cell labeling and organelle tracking. *Advanced Materials* 16:961 - 966.
- Dmitri V. Talapin, Stephan Haubold, Andrey L. Rogach, Andreas Kornowski, Markus Haase, and Horst Weller. 2001. A Novel Organometallic Synthesis of Highly Luminescent CdTe Nanocrystals *Journal Physical Chemistry B* 105: 2260-2263.
- Dmitri V. Talapin, Ivo Mekis, Stephan Goltzinger, Andreas Kornowski, Oliver Benson, and Horst Weller. 2004 CdSe/CdS/ZnS and CdSe/ZnSe/ZnS Core-Shell-Shell Nanocrystals. *Journal Physical Chemistry B* 108: 18826-18831.
- Dongzhi Yang, Shukun Xu, Qifan Chen, Wenxing Wang. A simple organic synthesis for CdS and Se-doped CdS nanocrystals. 2007. *Colloids and Surfaces A: Physicochemical Engineering Aspects* 299:153–159.

- Dubertret, B. Skourides, P. Norris, D. J. Noireaux, V. Brivanlou, A. H. Libchaber, A. 2002. In vivo imaging of quantum dots encapsulated in phospholipid micelles. *Science* 298 : 1759 - 1762.
- Eunjoo Jang, Shinae Jun, Lyongsun Pu.2003. High quality CdSeS nanocrystals synthesized by facile single injection process and their electroluminescence. *Chemical Communications* 10 : 2964-2965.
- Fellers T.J.,Davidson M.W. 2007. *Introduction to Confocal Microscopy*. Olympus Fluoview Resource Center, National High Magnetic Field Laboratory.
- Frangioni JV. 2003. In vivo near-infrared fluorescence imaging. *Current Opinion in Chemical Biology* 7:626–634.
- Gerion D, Parak WJ, Williams SC, Zanchet D, Micheel CM, Alivisatos AP.2002. Sorting fluorescent nanocrystals with DNA. *Journal of American Chemical Society* 124:7070–7074.
- Goldstein, A N. Echer, C M. Alivisatos, A P. 1992 . Melting in semiconductor nanocrystals. *Science*. 256 :1425-1427.
- Hanaki K, Momo A, Oku T, Komoto A, Maenosono S, Yamaguchi Y. 2003. Semiconductor quantum dot/albumin complex is a long-life and highly photostable endosome marker. *Biochemical and Biophysical Research Communications* 302:496–501.
- Hasegawa U, Nomura SIM, Kaul SC, Hirano T, Akiyoshi K. 2005. Nanogel-quantum dot hybrid nanoparticles for live cell imaging. *Biochemical and Biophysical Research Communications* 331:917–921.
- Heyduk T. 2002 Measuring protein conformational changes by FRET/ LRET. *Current Opinion in Biotechnology* 13:292– 296.
- Hui Peng, Lijuan Zhang, Christian Soeller, Jadranka Travas-Sejdic. 2007. Preparation of water-soluble CdTe/CdS core/shell quantum dots with enhanced photostability. *Journal of Luminescence* 127:721–726.
- Huifeng Qian, Chaoqing Dong, Jinliang Peng, Xin Qiu, Yuhong Xu, and Jicun Ren. 2007. High-Quality and Water-Soluble Near-Infrared Photoluminescent CdHgTe/CdS Quantum Dots Prepared by Adjusting Size and Composition. *Journal Physical Chemistry C* 111: 16852-16857.
- Ireneusz Strzalkowski, Sharad Joshi, C. R. Crowell. 1976. Dielectric constant and its temperature dependence for GaAs, CdTe, and ZnSe. *Applied Physics Letters* 28 : 350.
- Ivo Mekis, Dmitri V. Talapin, Andreas Kornowski, Markus Haase, and Horst Weller. 2003. One-Pot Synthesis of Highly Luminescent CdSe/CdS Core-Shell

Nanocrystals via Organometallic and “Greener” Chemical Approaches. *Journal Physical Chemistry B* 107:7454-7462.

Jaiswal J.K., Mattoussi H., Mauro J.M., Simon S.M. 2003. Long-term multiple color imaging of live cells using quantum dot bioconjugates. *Nature Biotechnology* 21:47–51.

Jasmina Lovrić . Hassan S. Bazzi . Yan Cuie . Genevieve R. A. Fortin . Françoise M. Winnik.2005.Dusica Maysinger. Differences in subcellular distribution and toxicity of green and red emitting CdTe quantum dots. *Journal of Molecular Medicine* 83: 377–385.

Juandria V. Williams. 2008. *Hydrothermal Synthesis and Characterization of Cadmium Selenide Nanocrystals*. University of Michigan.

Kagan CR, Murray CB, Nirmal M, Bawendi MG. 1996. Electronic energy transfer in CdSe quantum dot solids. *Physics Review Letters* 76: 1517–1520.

Lee LY, Ong SL, Hu JY, Ng WJ, Feng YY, Tan XL, 2004. Use of semiconductor quantum dots for photostable immunofluorescence labeling of *Cryptosporidium parvum*. *Applied Environmental Microbiology* 70:5732–5736.

Lim YT, Kim S, Nakayama A, Stott NE, Bawendi MG, Frangioni JV. 2003. Selection of quantum dot wavelengths for biomedical assays and imaging. *Molecular Imaging* 2:50–64.

Mani Ethayaraja, Chettiannan Ravikumar, Devarajan Muthukumar, Kanchan Dutta, and Rajdip Bandyopadhyaya. 2007. CdS-ZnS Core-Shell Nanoparticle Formation: Experiment, Mechanism, and Simulation. *Journal Physical Chemistry C* 111: 3246-3252.

Maoquan Chu, Xiaoyan Shen and Guojie Liu.2006. Microwave irradiation method for the synthesis of water-soluble CdSe nanoparticles with narrow photoluminescent emission in aqueous solution. *Nanotechnology* 17:444–449

Mark Green,Hannah Harwood,a Claire Barrowman, Paula Rahman,Alex Eggeman,Fred Festry, Peter Dobson and Tony Ng. 2007. A facile route to CdTe nanoparticles and their use in bio-labelling. *Journal of Materials Chemistry* 17: 1989–1994.

Michael J. Bowers II, James R. McBride, and Sandra J. Rosenthal. 2005. White-Light Emission from Magic-Sized Cadmium Selenide Nanocrystals. *Journal of American Chemical Society* 127:15378-15379.

Moazzam Ali, Soma Chattopadhyay, Angshuman Nag,Akshay Kumar, Sameer Sapra, S Chakraborty, D.D.Sarma. 2007. White-light emission from a blend of CdSeS nanocrystals of different Se:S ratio. *Nanotechnology* 18 : 075401.

Mosmann T. 1983. Rapid colorimetric assay for cellular growth and survival: application to proliferation and cytotoxicity assays. *Journal of immunological methods* 65: 55–63.

- Nikolai Gaponik, Dmitri V. Talapin, Andrey L. Rogach, Kathrin Hoppe, Elena V. Shevchenko, Andreas Kornowski, Alexander Eychmüller, and Horst Weller. 2002. Thiol-Capping of CdTe Nanocrystals: An Alternative to Organometallic Synthetic Routes. *Journal Physical Chemistry B* 106: 7177-7185.
- Parvesh Sharma, Scott Brown, Glenn Walte , Swadeshmukul Santra, Brij Moudgil. 2006 Nanoparticles for bioimaging. *Advances in Colloid and Interface Science* 123:471–485.
- Pathak S, Choi SK, Arnheim N, Thompson ME. 2001. Hydroxylated quantum dots as luminescent probes for in situ hybridization. *Journal of American Chemical Society* 123:4103–4104.
- Pawley J.B. 2006. *Handbook of Biological Confocal Microscopy (3rd ed. ed.)*. Berlin: Springer.
- Pinuad, F. King, D. Moore, H.-P. Weiss, S. 2004. Bioactivation and cell Targeting of Semiconductor CdSe / ZnS Nanocrystals with Phytochelatin – Related Peptides. *Journal of American Chemical Society* 126 : 6115–6123.
- Qiang Wang, Daocheng Pan, Shichun Jiang, Xiangling Ji, Lijia An, and Bingzheng Jiang. 2005. A New Two-Phase Route to High-Quality CdS Nanocrystals. *Chemistry European Journal* 11: 3843 – 3848.
- Rieger S, Kulkarni RP, Darcy D, Fraser SE, Koster RW. 2005. Quantum dots are powerful multipurpose vital labeling agents in zebrafish embryos. *Dev Dyn* 234:670–81.
- Riegler J, Nann T. 2004. Application of luminescent nanocrystals as labels for biological molecules. *Analytical and Bioanalytical Chemistry* 379:913–919.
- S. Shankara Narayanan and Samir Kumar Pal. 2006. Aggregated CdS Quantum Dots: Host of Biomolecular Ligands. *Journal Physical Chemistry B* 110 : 24403-24409.
- Sander F. Wuister, Ingmar Swart, Floris van Driel, Stephen G. Hickey, and Celso de Mello Donega. 2003. Highly Luminescent Water-Soluble CdTe Quantum Dots. *Nano Letters* 3 : 503 - 507.
- Selvin PR. 2000 The renaissance of fluorescence resonance energy transfer. *Nature Structural Biology* 7:730–734.
- Streetman, Ben G., Sanjay Banerjee. 2000. *Solid State electronic Devices (5th edition ed.)* Prentice Hall.
- Sung Ju Cho, Dusica Maysinger, Manasi Jain, Beate Röder, Steffen Hackbarth, and Francüoise M. Winnik. 2007. Long-Term Exposure to CdTe Quantum Dots Causes Functional Impairments in Live Cells. *Langmuir* 23:1974-1980.

- Tian-Long Zhang, Yun-Sheng Xia, Xue-Lian Diao and Chang-Qing Zhu. 2008. Preparation and formation mechanism of strong violet luminescent CdS quantum dots by using a ligand exchange strategy. *Journal of Nanoparticle Research* 10 : 59–67.
- Timothy Jamieson, Raheleh Bakhshi, Daniela Petrova, Rachael Pocock, Mo Imani, Alexander M. Seifalian. 2007 Biological applications of quantum dots. *Biomaterials* 28:4717-4732.
- Tully E, Hearty S, Leonard P, O’Kennedy R. 2006. The development of rapid fluorescence-based immunoassays, using quantum dot-labelled antibodies for the detection of *Listeria monocytogenes* cell surface proteins. *International Journal of Biological Macromolecules* 39:127–134.
- V. L. Colvin, M. C. Schlamp, A. P. Alivisatos. 1994. Light-emitting diodes made from cadmium selenide nanocrystals and a semiconducting polymer. *Nature* 370: 354 – 357.
- Wang, X. S. Dykstra, T. E. Salvador, M. R. Manners, I. Scholes, G. D. Winnik, M. A. 2004. Surface passivation of luminescent colloidal quantum dots with poly(dimethylaminoethyl methacrylate) through a ligand exchange process *Journal of American Chemical Society* 126 : 7784 – 7785.
- Wen Jiang, Anupam Singhal, Jianing Zheng, Chen Wang, and Warren C. 2006. W. Chan. Optimizing the Synthesis of Red- to Near-IR-Emitting CdS-Capped CdTe_xSe_{1-x} Alloyed Quantum Dots for Biomedical Imaging. *Chemical Materials* 18:4845-4854.
- William W. Yu , Emmanuel Chang , Rebekah Drezek , Vicki L. Colvin. 2006. Water-soluble quantum dots for biomedical applications. *Biochemical and Biophysical Research Communications* 348:781–786.
- Xianfeng Chen , John L. Hutchison , Peter J. Dobson , Gareth Wakefield . 2008. A one-step aqueous synthetic route to extremely small CdSe nanoparticles. *Journal of Colloid and Interface Science* 319:140–143.
- Xiao Y, Barker PE. 2004. Semiconductor nanocrystal probes for human metaphase chromosomes. *Nucleic Acids Research* 32 : 28 – 33.
- Y. Charles Cao. and Jianhui Wang. 2004. One-Pot Synthesis of High-Quality Zinc-Blende CdS Nanocrystals. *Journal of American Chemical Society* 126 : 14336-14337.
- Yan Li, Fuzhi Huang, Qingmin Zhang, Zhennan Gu. 2000. Solvothermal synthesis of nanocrystalline cadmium sulfide. *Journal Of Materials Science* 35:5933 – 5937.
- Yang, H. Holloway, P. H. Santra, S. 2004. Water-soluble silica-overcoated CdS : Mn/ZnS semiconductor quantum dots. *Journal Chemical Physics* 121 : 7421–7426.

- Ying Wang, Zhiyong Tang, and Nicholas A. Kotov. 2005 Bioapplication of nanosemiconductors. *Nanotoday* 8:21-30.
- Yun-Sheng Xia, Chang-Qing Zhu. 2007. Aqueous synthesis of luminescent magic sized CdSe nanoclusters. *Materials Letters* 62 : 2103 – 2105.
- Z. Adam Peng and Xiaogang Peng. 2001. Formation of High-Quality CdTe, CdSe, and CdS Nanocrystals Using CdO as Precursor. *Journal of American Chemical Society* 123: 183-184.
- Zhenyu Gu, Lei Zou, Zheng Fang, Weihong Zhu and Xinhua Zhong. 2008. One-pot synthesis of highly luminescent CdTe/CdS core/shell nanocrystals in aqueous phase. *Nanotechnology* 19: 135604 -135612
- Zhu L., Ang S., Liu W.T. 2004. Quantum dots as a novel immunofluorescent detection system for *Cryptosporidium parvum* and *Giardia lamblia*. *Applied Environmental Microbiology* 70:597–598.
- Yang L.J., Li Y.B. 2006. Simultaneous detection of *Escherichia coli* O157: H7 and *Salmonella Typhimurium* using quantum dots as fluorescence labels. *Analyst* 131:394–401.
- Yang, H. Holloway, P. H. Santra, S. 2004. Water-soluble silica-overcoated CdS : Mn/ZnS semiconductor quantum dots. *Journal of Chemical Physics* 121 : 7421–7426.
- Ying Wang, Zhiyong Tang, and Nicholas A. Kotov. 2005 Bioapplication of nanosemiconductors. *Nanotoday* 8:21-30.
- Z. Adam Peng and Xiaogang Peng. 2001. Formation of High-Quality CdTe, CdSe, and CdS Nanocrystals Using CdO as Precursor. *Journal of American Chemical Society* 123: 183-184.
- Zhu L, Ang S, Liu WT. 2004. Quantum dots as a novel immunofluorescent detection system for *Cryptosporidium parvum* and *Giardia lamblia*. *Applied Environmental Microbiology* 70:597–598.